



CZECH TECHNICAL UNIVERSITY IN PRAGUE
FACULTY OF MECHANICAL ENGINEERING

Department of Automotive, Combustion Engine and Railway
Engineering



Master Thesis

Planetary Gearbox for Electric Vehicle

Author : Samed Ali Akköse

Supervisor : doc. Dr. Ing. Gabriela Achtenová

Prague, 2020

I. Personal and study details

Student's name: **Akköse Samed Ali** Personal ID number: **484094**
Faculty / Institute: **Faculty of Mechanical Engineering**
Department / Institute: **Department of Automotive, Combustion Engine and Railway Engineering**
Study program: **Master of Automotive Engineering**
Branch of study: **Advanced Powertrains**

II. Master's thesis details

Master's thesis title in English:

Planetary gearbox for electric vehicle

Master's thesis title in Czech:

Planetová převodovka pro elektrické vozidlo

Guidelines:

- 1) Make a review of powertrains of serially produced electric vehicles. Also provide a review of patented solution of EV powertrains.
- 2) Choose the parameters of passenger EV, for which you will design the transmission. Choose right energy source.
- 3) Propose several variants of transmission and make a guess of efficiency, mass and dimensions. Minimally one variant has to be planetary one.
- 4) For chosen planetary variant prepare a CAD model and basic necessary strength calculations. Make a fabrication drawing of one part chosen by the tutor.

Bibliography / sources:

- [1] Lino Guzzela, Antoniol Sciarretta:
Vehicle Propulsion and Systems, Introduction to Modeling and Optimization, Second Edition
Springer-Verlag Berlin Heidelberg, 2007
ISBN 978-3-540-74691-1
- [2] Harald Naunheimer, Bernd Bertsche, Joachim Ryborz, Wolfgang Novak
Automotive Transmissions, Fundamentals, Selection, Design and Application Second Edition
Springer Heidelberg Dordrecht London New York 2011

Name and workplace of master's thesis supervisor:

doc. Dr. Ing. Gabriela Achtenová, Department of Automotive, Combustion Engine and Railway Engineering, FME

Name and workplace of second master's thesis supervisor or consultant:

Ing. Filip Hostaš, Ricardo Prague

Date of master's thesis assignment: **09.03.2020** Deadline for master's thesis submission: **14.08.2020**

Assignment valid until: _____

doc. Dr. Ing. Gabriela Achtenová
Supervisor's signature

doc. Ing. Oldřich Vitek, Ph.D.
Head of department's signature

prof. Ing. Michael Valášek, DrSc.
Dean's signature

III. Assignment receipt

The student acknowledges that the master's thesis is an individual work. The student must produce his thesis without the assistance of others, with the exception of provided consultations. Within the master's thesis, the author must state the names of consultants and include a list of references.

_____ .
Date of assignment receipt

Student's signature



Annotation

Author	: Samed Ali Akköse
Title	: Planetary Gearbox for Electric Vehicle
Academic Year	: 2019/2020
Programme	: Master of Automotive Engineering
Major	: Advanced Powertrains
Supervisor	: doc. Dr. Ing. Gabriela Achtenová
Abstract	: This thesis consists of research on battery electric vehicles currently available on the market and their powertrains, reviews of patented solutions of electric vehicle powertrains, calculations of longitudinal dynamics of the selected vehicle and its design parameters, three variants of powertrains and their mass, efficiency and dimension estimations, calculation of a planetary gearbox system and the strength calculation results. The thesis also includes a 2D CAD model of the assembly and fabrication drawing of the sun shaft, 3D CAD model of the planetary gearbox and results of strength calculations on Ricardo Company's SABR/GEAR software.
Keywords	: Electric Vehicle, Powertrain, Vehicle Dynamics, Planetary Gearset, Computer Aided Design (CAD)
Number of Pages	: 91
Number of Figures	: 66
Number of Tables	: 18



Declaration

I hereby declare that the thesis ‘Planetary Gearbox for Electric Vehicle’ is based on my own work. All ideas, major views and data from different resources by other authors were only used as a reference and/or research purpose. I am the sole author of the thesis and that neither any part of this thesis nor the whole of the thesis has been submitted for a degree to any other University or Institution.

In Prague

Samed Ali Akköse



Acknowledgements

I would like to thank my thesis supervisor Mrs. Gabriela ACHTENOVÁ for her great understanding and patience.

I also would like to thank to Mr. Roman ČERMÁK for his help and directing me to find a correct subject according to my interests. Whenever I have a problem to solve, his door is always open to me.

From the first letter to the printing process, I would like to thank Mr. Karel FOŘTL. Without his help and time, thesis would not be completed.

With his great help and patience, I also would like to thank Mr. Filip HOSTAŠ, with his great support, solve my problems, his time and guidance.

I would like to thank to Mr. Sami KULBUL for his motivational help.

Finally, my special thanks belong to my parents for their encouragement, love and their belief to me.



Table of Contents

1. Introduction.....	14
2. Review of Powertrains of Serially Produced EV's	16
2.1. Battery Electric Vehicles Currently Available on the market.....	17
2.1.1. <i>Audi e-tron.....</i>	18
2.1.2. <i>BMW i3.....</i>	18
2.1.3. <i>Citroën C-Zero</i>	19
2.1.4. <i>Chevrolet Bolt EV.....</i>	19
2.1.5. <i>Tesla</i>	20
2.1.6. <i>Nissan LEAF</i>	21
2.1.7. <i>Jaguar I-Pace.....</i>	21
2.1.8. <i>Volkswagen e-Golf.....</i>	22
2.2. General Review of the Transmissions.....	23
2.3. Patented Solutions of Electric Vehicle Powertrains	26
2.3.1. <i>International Patent Classification (IPC).....</i>	26
2.3.2. <i>Cooperative Patent Classification System (CPC).....</i>	26
2.3.3. <i>KR101971189B1 , Transmission of Electric Vehicle</i>	28
2.3.4. <i>WO2019214995A1 , Multi-speed Planetary Transmission.....</i>	29
2.3.5. <i>WO2019115204A1, Electric Drive for a Motor Vehicle.....</i>	30
2.3.6. <i>WO2019091719A1 , Transmission for an Electric Vehicle</i>	31
2.3.7. <i>US20160003351A1, Two-Speed Transmission for Vehicle.....</i>	32
3. Vehicle Parameters and Energy Source Selection	33
3.1. Parameters of Chevrolet Bolt EV	33
3.2. Longitudinal Dynamics Calculation	34
3.2.1. <i>Rolling Resistance</i>	34
3.2.2. <i>Air Drag</i>	34
3.2.3. <i>Acceleration Resistance</i>	35
3.2.4. <i>Gradient Resistance</i>	35
3.3. Total Driving Resistance	36
3.3.1. <i>YASA P-400 RS Electric Motor.....</i>	37



4. Efficiency, Mass and Dimension Comparison of the Transmission Systems ...	45
4.1. Efficiency and Losses.....	47
4.1.1. <i>Lubrication Losses</i>	47
4.1.2. <i>Meshing (Tooth-Friction) Losses</i>	47
4.1.3. <i>Losses in Bearings.....</i>	48
4.2. Mass and Dimension Estimation	53
4.2.1. <i>Mass Comparison of the Selected Transmission Systems</i>	53
4.2.2. <i>Dimension Comparison of the Selected Transmission Systems</i>	54
5. The Planetary Gearset Design	56
5.1. Selection : Planetary Single Speed Reduction.....	56
5.2. The Ratio and The Planet Diameters Calculation	58
5.2.1. <i>The Basic Ratio of the Planetary Gearing</i>	59
5.2.2. <i>Pitch Diameter and Teeth Number Calculation of the Planetary Gearset Components</i>	60
5.2.3. <i>Pitch Diameter and Teeth Number Calculations of the Final Drive</i>	64
5.3. Strength Calculations of The Gear Meshes with SABR Software	67
5.3.1. <i>Duty Cycle</i>	67
5.3.2. <i>Material Properties of the Components</i>	68
5.3.3. <i>Sun/Planet Mesh Results</i>	70
5.3.4. <i>Planet/Annulus(Ring) Mesh Results.....</i>	73
5.3.5. <i>Final Drive/Pinion Mesh Results</i>	75
5.4. Strength Calculations of the Components with SABR Software	78
5.4.1. <i>Bearing Selection</i>	79
5.4.2. <i>Bearing Life and Temperature</i>	80
5.4.3. <i>Deflections on Shaft</i>	81
5.4.4. <i>Stresses Applied on Shaft</i>	84
6. Conclusion	86
7. References.....	89



List of Figures

Fig. 1	Electric car Deployment in Selected Countries, 2013-2018 [1].....	14
Fig. 2	Expected BEV Sales in the years 2025 and 2030 [1].....	15
Fig. 3	BEV Configuration [4]	16
Fig. 4	BEV Anatomy [U.S Department of Energy].....	17
Fig. 5	Audi e-tron (left),Transmission System(right) 2018 [5] [6].....	18
Fig. 6	BMW i3 (left), Transmission System (right) [6] [8]	18
Fig. 7	Citroën C-Zero (left) and it ´s transmission (right) [6] [9]	19
Fig. 8	Chevrolet Bolt EV (left) the Electric Drive Unit (right) [6][10]	19
Fig. 9	Tesla Model 3 (left) , Transmission System (right) [6] [11]	20
Fig. 10	Transmission System (middle), Model X(left), Model S(right) [6] [12] [13]	20
Fig. 11	Nissan LEAF (left), Transmission System (right) [6] [14]	21
Fig. 12	Jaguar I-Pace (left) , Transmission System (right) [6] [15].....	21
Fig. 13	Volkswagen e-Golf (left), Electric Drive Unit (right) [6] [16].....	22
Fig. 14	Electric Drive Unit Disassembly of VW e-Golf [6]	22
Fig. 15	Classification Research for Planetary Transmission [16].....	27
Fig. 16	The Patented Transmission For Electric Vehicle and Power Flow[17]	28
Fig. 17	Multi Speed Planetary Transmission for Vehicle and Power Flow [18].....	29
Fig. 18	WO2019115204A1 Patent Design and the Power Flow [19].....	30
Fig. 19	WO201909179A1 Patent Design and Power Flow [20]	31
Fig. 20	US20160003351A1 Patent Design and Power Flow [21]	32
Fig. 21	Chevrolet Bolt 2020 Front View [22].....	33
Fig. 22	The Forces Acting on the Vehicle, Uphill Movement.....	35
Fig. 23	YASA P-400 RS PMSMElectric Motor [26]	37
Fig. 24	The Chosen YASA Motor Characteristics	38
Fig. 25	Tractive Force vs. RPM.....	39
Fig. 26	Velocity vs. Time	40
Fig. 27	Acceleration vs. Time	40
Fig. 28	Distance vs. Time	41
Fig. 29	Acceleration vs. Velocity	41
Fig. 30	RPM vs. Velocity	42
Fig. 31	RPM vs. Time.....	42



Fig. 32	Planetary Reduction With Additional Simple Parallel Gear Step	45
Fig. 33	Two Stage Parallel Shaft, Layshaft Transmission.....	46
Fig. 34	Planetary gear reductor with Compound Planets	46
Fig. 35	Efficiency Calculation of The Variant One	50
Fig. 36	Efficiency Calculation of the Variant Three.....	51
Fig. 37	Configuration of the First Variant of the Selected Transmissions	54
Fig. 38	Configuration of the Second Variant of the Selected Transmissions.....	55
Fig. 39	Configuration of the Third Variant of the Selected Transmissions.....	55
Fig. 41	Configuration of Variant Three	57
Fig. 40	Configuration of the Selected Variant	57
Fig. 42	Designation of Subscripts and Superscript.....	58
Fig. 43	Illustration for Showing the Pitch Diameters of the Components.....	60
Fig. 44	Illustration of Final Drive and the Pinion Pitch Diameters	65
Fig. 45	Screenshot of Ricardo Software SABR.....	68
Fig. 46	S-N Curve of 27MnCr5 for Bending Stress and Contact Stress [34].....	69
Fig. 47	Basic Geometry Features in Sun/Planet Configuration in SABR/GEAR	70
Fig. 48	The Inputs for Microgeometry and Backlash in SABR/GEAR	70
Fig. 49	Results for Bending in Nominal(Above) and Maximum Torque(Below).....	71
Fig. 50	Results for Contact in Nominal(Above) and Maximum Torque(Below).....	72
Fig. 51	Results for Bending Stress in Nominal Torque	73
Fig. 52	Results for Bending Stress in Maximum Torque	74
Fig. 53	Results for Contact in Nominal(Above) and Maximum Torque(Below).....	74
Fig. 54	Results for Bending in Nominal(Above) and Maximum Torque(Below).....	76
Fig. 55	Results for Contact Stress in Nominal Torque	77
Fig. 56	Results For Contact Stress in Maximum Torque.....	77
Fig. 57	Screenshot from the SABR Software	78
Fig. 58	Locations of The Bearings in the Assembly.....	79
Fig. 59	Maximum Bearing Temperature Simulation	80
Fig. 60	LOMA and CD Displacement in FD and Pinion Mesh.....	81
Fig. 61	Slopes and Deflections of the Differential with Respect to Location	82
Fig. 62	Slopes and Deflections of the Carrier with Respect to Location.....	83
Fig. 63	Results of Stresses Applied on Shafts in SABR Software	85



Fig. 64 Life Conditions of Bearings on SABR Software	85
Fig. 65 The Planetary Gearbox For Electric Vehicle in CATIA V5	87
Fig. 66 Front and Side View Of the Powertrain Design	88



List of Tables

Tab. 1	Kinematic Schemes of the Transmissions Regarding to the Model.....	23
Tab. 2	Specifications of Chevrolet Bolt 2020 [22].....	33
Tab. 3	Input Parameters for Calculation of Total Driving Resistance.....	36
Tab. 4	YASA P-400 RS Specifications	38
Tab. 5	Reference Values of Meshing Friction Losses [29]	47
Tab. 6	Efficiency Estimation of the Variant 1	51
Tab. 7	Efficiency Estimations of Variant 2 and 3.....	52
Tab. 8	Required Parameters for Centre Distance Calculation	64
Tab. 9	Results of the Planetary Gearset Design Calculations.....	66
Tab. 10	Ricardo's Suggested Duty Cycle Strategy for the Current Gearbox	67
Tab. 11	Material Properties of 27MnCr5.....	69
Tab. 12	Entered Duty Cycle Properties For Sun/Planet Mesh	71
Tab. 13	Entered Duty Cycle Properties For Planet/Ring Mesh.....	73
Tab. 14	Entered Duty Cycle Properties for Final Drive / Pinion Mesh.....	75
Tab. 15	The Bearings Which are Used in The Assembly	79
Tab. 16	The Applied Stress/ Amount of Damage on Bearings	80
Tab. 17	Maximum Radial Deflection By Load Case.....	81
Tab. 18	The von Misses Stresses Applied on Shafts	84



Acronyms

AC	Alternating Current
AWD	All-Wheel Drive
BEV	Battery Electric Vehicle
CPC	Cooperative Patent Classification
EDU	Electric Drive Unit
EV	Electric Vehicle
FD	Final Drive
IPC	International Patent Classification
ISO	International Organization for Standardization
LOAMA	Load of Action Misalignment
PCD	Pitch Circle Diameter
PGS	Planetary Gear Set
PMSM	Permanent Magnet Synchronous Motor
RWD	Rear Wheel Drive
SUV	Sport Utility Vehicle



1. Introduction

General Overview to Electric Vehicles

An electric vehicle (EV) uses an electric motor as a power source. After the invention of the storage battery in 1850's and the improvements in the area made the production of the electric vehicle possible and the first application used in Paris in 1881.

In the early years of the automotive industry, the electric vehicles were in a competition with petroleum-fueled cars but their low top speeds, high costs, the short range because of the inefficiency of the batteries and the discovery of the large amount of fossil fuels in 1920's caused a reduction of the prices in the gasoline. As a result, the use of the electric vehicles declined.

In the recent years, the electric vehicles become an important research subject. Especially in the last decade the electric vehicles started to be more dominant on the market again. Decreasing of the fossil fuels and increase in the gas prices, recent improvements in the battery and power electronic technologies and since the battery electric vehicles have zero tailpipe emissions in comparison with the petroleum-fueled cars can be shown as the main reasons for the explanation why the electric vehicles are becoming more popular.

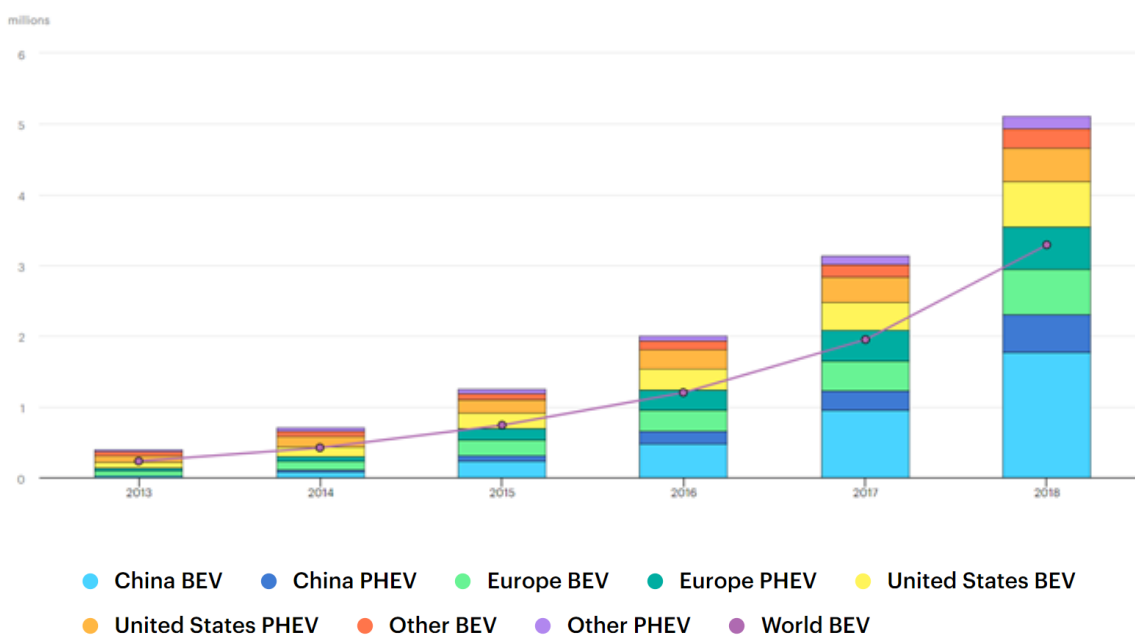


Fig. 1 Electric car Deployment in Selected Countries, 2013-2018 [1]



From the actual sales data, the electric car deployment is increasing [1]. The Figure 1 shows that, in 2018 there was a 63% increase in the electric vehicle deployment in the world. Four-wheel, battery electric vehicle (BEV) worldwide, amounted to approximately three million units. Since it is compared, this number is coming to less than 3% of the global total automobile sales. Also, it could be seen from the Figure 2 that by the year 2030 it is expected that the Battery Electric Vehicle deployment would reach up to 25 million units.

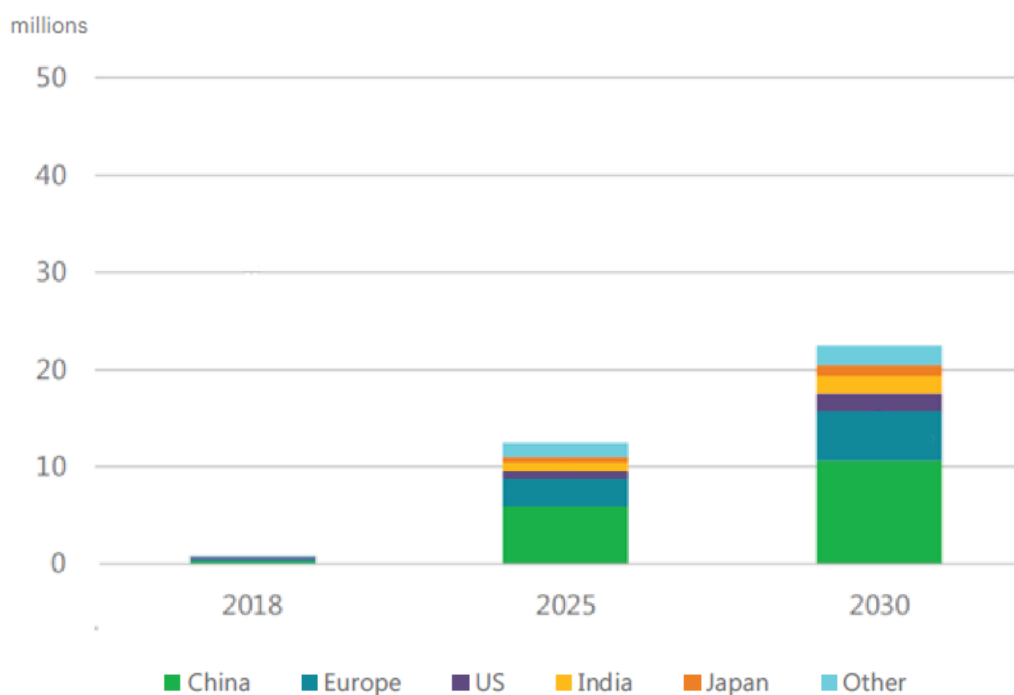


Fig. 2 *Expected BEV Sales in the years 2025 and 2030 [1]*

Since it is seen from the actual sales data and the future estimations, the battery electric vehicles will be more frequent on the market and in the streets in global scale. Since the vehicles are running with the electricity, the efficiency of the powertrain parts has critical importance for the battery life.



2. Review of Powertrains of Serially Produced EV's

The electric vehicles which are using only the batteries as the power source are called as Battery Electric Vehicle (BEV). Compared with the conventional combustion engine vehicles, the battery electric vehicles (BEV) are simpler and easier to operate because they do not have complex transmissions. Most battery electric vehicles have single speed transmission. Also, the BEV's does not have exhaust systems. It means no exhaust after treatment device needed in a battery electric vehicle. The battery electric vehicles are consisting of;

a. Battery Pack: This is the energy source of the vehicle which it will be used in drive, heat & cooling operations and running the light of accessories. Lithium-ion batteries are found in most of the modern EV's today. [3]

b. Power Inverter: Since the electric vehicle has AC motor, the energy from the battery should be converted into AC to be used. The inverter also works during the regenerative braking to modify the alternative current into direct current.

c. Electric Motor : This is the electric machine which converts the electrical energy into mechanical energy to use in drive.

d. Transmission : This is the machine which provides controlled application of the power. In the battery electric vehicles mostly Single Speed Transmissions are used. Single speed transmission is more advantageous because there will be no need for shifting of gears and no need of a clutch.

e. Charging Port : Charging port is the location where the electrical energy enters the car, much like the access port to the gas tank in an internal combustion engine (ICE).

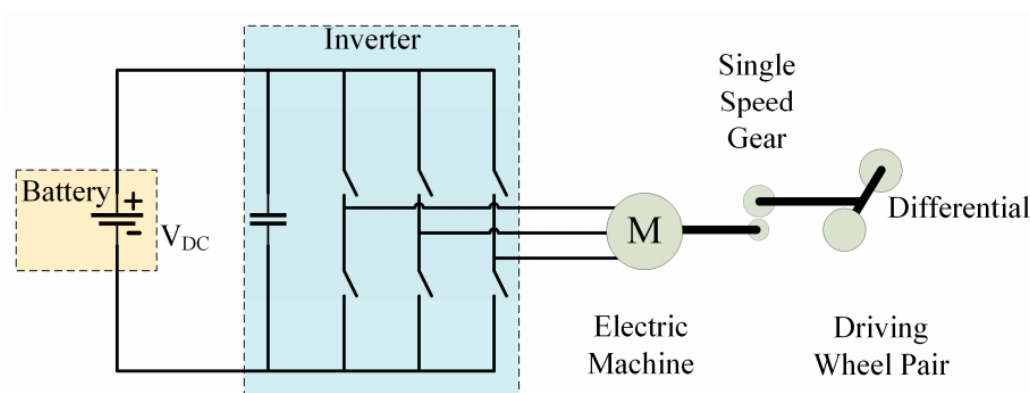


Fig. 3 BEV Configuration [4]

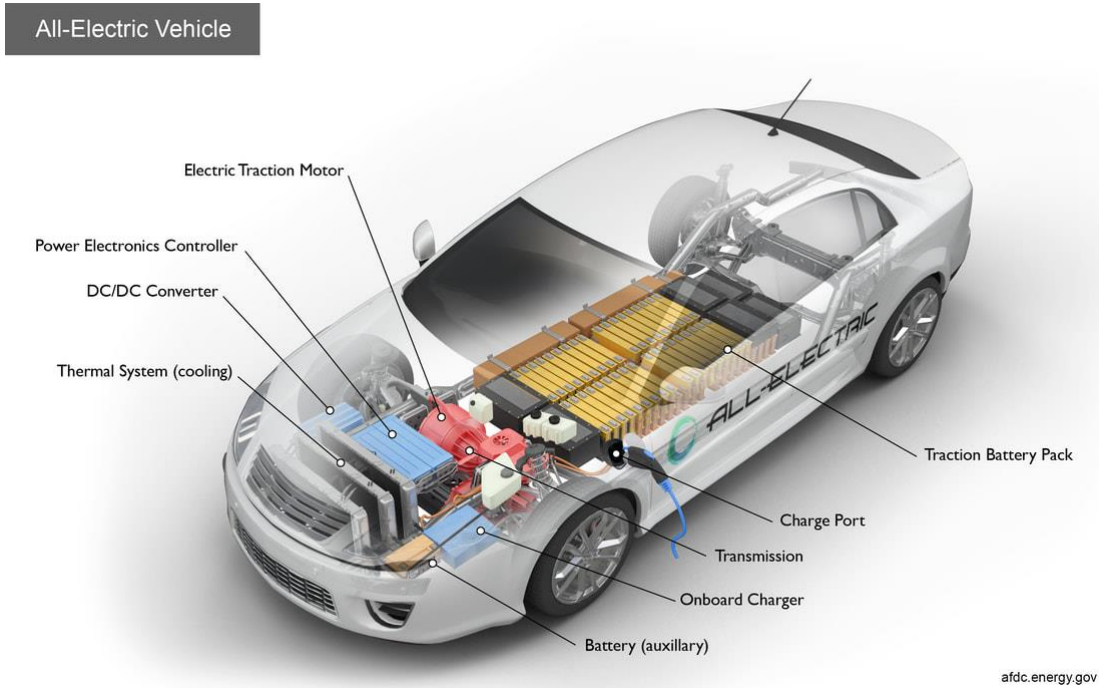


Fig. 4 BEV Anatomy [U.S Department of Energy]

In the last decades so many automotive manufacturers started to introduce EV's and they have entered to the automotive market. Those vehicles range are related with their battery capacity. Typical range of the BEV is 100km to 250km regarding on the driving and the environmental conditions [2].

2.1. Battery Electric Vehicles Currently Available on the market

In this project, to be able to make a design of a powertrain, it is necessary to make a research on the vehicles which are currently available on the market. Each car has different aspects that with the data available the inspiration could be helpful for the vehicle parameters selection.

The vehicles are selected according to their market sales and sorted alphabetically.



2.1.1. Audi e-tron

Since the electric car industry improves, each brand joins the car market with a new alternative. Audi e-tron is the all-electric SUV, the first mass production electric car of the company. It is being produced since 2018.

Audi e-tron uses planetary reduction on the front axle with additional simple parallel gear step to differential.



Fig. 5 Audi e-tron (left), Transmission System(right) 2018 [5] [6]

2.1.2. BMW i3

BMW i3 is the first mass produced electric vehicle of the company and it is launched by the BMW's subcompany BMW i [7]. It is being produced since 2013 by the BMW Group in Plant Leipzig. In BMW i3 two stage parallel shaft with the compound gears on the countershaft is used. This design has rear wheel drive (RWD) layout.



Fig. 6 BMW i3 (left), Transmission System (right) [6] [8]



2.1.3. Citroën C-Zero

This model is the rebadged version of the Mitsubishi i-MiEV (Mitsubishi innovative Electric Vehicle). This vehicle is produced in Europe under the name of Citroën C-Zero and Peugeot iOn for the customers. Similar to BMW i3 design, also in this model a two stage parallel shaft with the compound gears on the countershaft is used.



Fig. 7 Citroën C-Zero (left) and its transmission (right) [6] [9]

2.1.4. Chevrolet Bolt EV

Chevrolet Bolt EV is the full electric production of the GM company. It is being produced since 2016. The vehicle is rebadged for the continental Europe and sold under the name Opel Ampera-e. In this model, two stage parallel shafts with compound gears on countershaft is used. Motor is coaxial with differential. It means the half shaft goes through the motor.

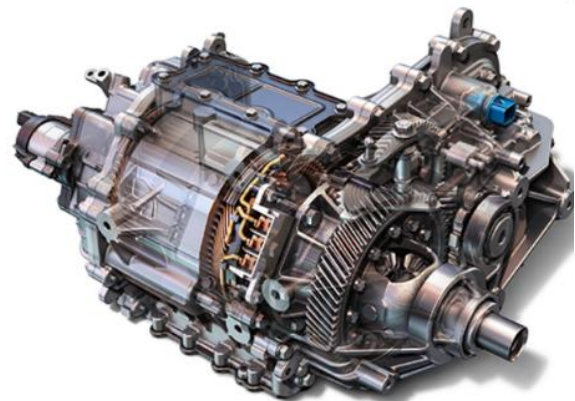


Fig. 8 Chevrolet Bolt EV (left) the Electric Drive Unit (right) [6][10]



2.1.5. Tesla

Tesla Inc. can be named as the pioneer of the electric car market. The company is focused on producing high performance electric vehicles. As it be can seen from their products on the market, they have three popular models. They are Model 3, Model X and Model S.

2.1.5.1. Tesla Model 3

Tesla Model 3 is the most popular model of the brand. It is produced since 2017.

In this model the two-stage parallel shaft with compound gears on the countershaft is used. This design has all-wheel-drive layout.



Fig. 9 Tesla Model 3 (left) , Transmission System (right) [6] [11]

2.1.5.2. Tesla Model X and Model S

Tesla Model S is the all-electric sedan and Tesla Model X is the luxury all electric SUV designed and produced by Tesla corporation. Both models have the all-wheel drive layout and has two electric motors in both rear and front axles. Also, in both Tesla S and Tesla X, same type of transmission single speed two stage parallel shaft is used.



Fig. 10 Transmission System (middle), Model X(left), Model S(right) [6] [12] [13]



2.1.6. Nissan LEAF

Nissan LEAF is the battery electric vehicle alternative of the company. It is produced since 2010 by the Japanese company Nissan Motor Company. Like its competitors, Nissan LEAF also has a single speed two stage parallel shaft with compound gears on the countershaft.



Fig. 11 Nissan LEAF (left), Transmission System (right) [6] [14]

2.1.7. Jaguar I-Pace

Jaguar I-Pace is the battery electric vehicle SUV which is produced by the company Jaguar Land Rover (JLR). Jaguar I-Pace is the first all-electric car of the company and produced since 2018. This vehicle uses two identical powertrains on both rear and front axles. The motor is coaxial with differential and there is a planetary gearset reduction.



Fig. 12 Jaguar I-Pace (left), Transmission System (right) [6] [15]



2.1.8. Volkswagen e-Golf

Volkswagen e-Golf is the all-electric version of the model VW Golf. It is produced since 2014. VW e-Golf also uses the system like their competitors BMW, Citroen, Nissan and Tesla; single speed two stage parallel shafts with compound gears on the countershaft.



Fig. 13 Volkswagen e-Golf (left), Electric Drive Unit (right) [6] [16]

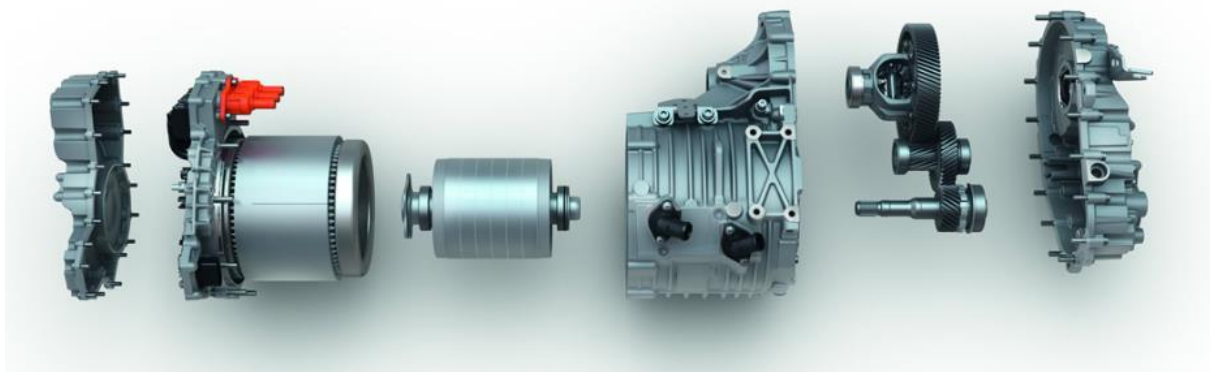


Fig. 14 Electric Drive Unit Disassembly of VW e-Golf [6]

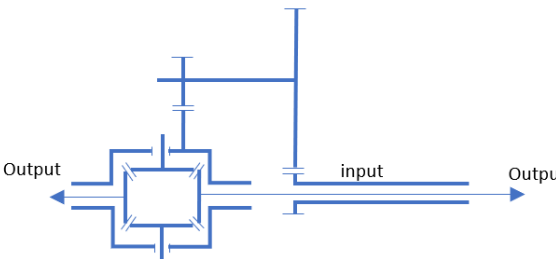
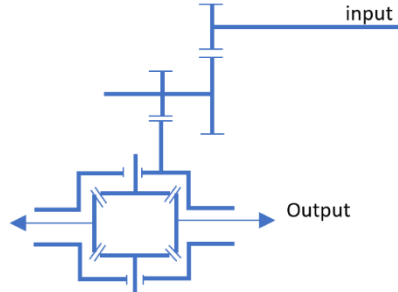
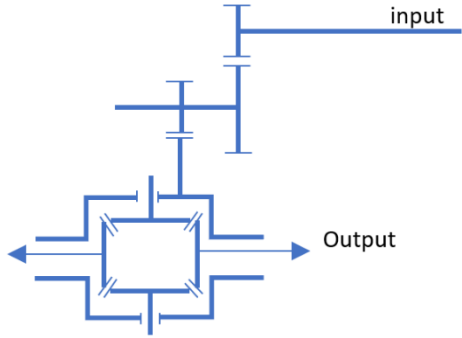
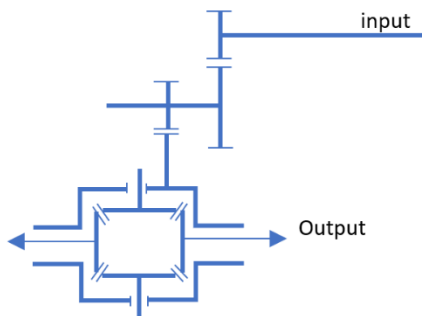


2.2. General Review of the Transmissions

Tab. 1 Kinematic Schemes of the Transmissions Regarding to the Model

Brand/Model	Type of Transmission	Kinematic Scheme
Audi e-tron	<p>Planetary Single Speed reduction. Sun is input, carrier is output, ring is stationary. There is additional simple parallel gear step to differential.</p>	
BMW i3	<p>Two stage parallel shaft with compound gears on the layshaft.</p>	
Citroen C-Zero	<p>Two stage parallel shaft with compound gears on the layshaft.</p>	



<p>Chevrolet Bolt EV</p>	<p>Two stage parallel shaft with compound gears on the layshaft. Motor is coaxial with differential. Half shaft goes through with the electric motor.</p>	
<p>Tesla Model 3</p>	<p>Two stage parallel shaft with compound gears on the layshaft.</p>	
<p>Tesla Model S-X</p>	<p>Two stage parallel shaft with compound gears on the layshaft.</p>	
<p>Nissan LEAF</p>	<p>Two stage parallel shaft with compound gears on the layshaft.</p>	



<p>Jaguar I-Pace</p>	<p>Planetary gear reductor with compound planets is used. Sun is input, carrier is output, ring is stationary. Sun is meshing with bigger planet and ring is meshing with smaller planets. Carrier is mounted to differential cage.</p>	
<p>VW e-Golf</p>	<p>Two stage parallel shaft with compound gears on the layshaft.</p>	



2.3. Patented Solutions of Electric Vehicle Powertrains

Before making a proper design for the powertrains which are going to be used in electric vehicles, the patented solutions and the new technological trends from the companies are also highly recommended. Because there is the risk of re-inventing the same design. Before making the research, it is important to know patent classification systems. By the help of the patent classification system, it is easier to make the research for the inventions which is the patent is correlated. To utilize the system the patent offices developed the hierarchical classification systems.

2.3.1. International Patent Classification (IPC)

The international Patent Classification serve as an instrument for orderly arrangement of the patent documents and helps the researcher to find the contemporary solutions of the related search field. All the International Patent Organisation Member companies' patents can be found. IPC revisions take place yearly.[14]

2.3.2. Cooperative Patent Classification System (CPC)

Cooperative Patent Classification System is developed by European Patent Office (EPO) and the United States Patent and Trademark office (USPTO). CPC system based on the IPC system although it is more detailed, and the CPC revisions take place monthly. Patent distributions are appointed in at least one grouping term and extra classification terms are used to give added specifications of the patent.

In the classification structure each term represents the category of the patent. Each patent has the specific symbol of "X00Y00/00". The first letter "X" represents the "section symbol" comprises the letters from "A (Human Necessities)" to "H (Electricity)" and "Y (Emerging Cross-Sectional Technologies)". After this letter the two-digit number gives the "Class Symbol". The final letter "Y" represents the "subclass symbol". After the subclass symbol it follows a one to four-digit "group" number, and at last, it follows with an at least two-digits "main group" number. This hierarchy helps the researcher to find similar concept technological solutions patents. [15]



Ranking of CPC

- Section (one letter A to H, and Y)
 - Class (two digits)
 - Subclass (one letter)
 - Group (one to four digits)
 - Main Group (at least three digits)

For the powertrain research the CPC ranking “**F16H2200/2005**” is used.

In this system it means;

- Section **F** (one letter A to H, and Y)
 - Class **16** (two digits)
 - Subclass **H** (one letter)
 - Group **2200** (one to four digits)
 - Main Group **2005**(at least three digits)

It can be seen the representation of the letters from the Fig. 15;

The screenshot shows a search interface with a search bar containing '2000' and a 'Search' button. The search results are displayed in a table with columns for 'Classification symbol' and 'Title and description'. The results are as follows:

Classification symbol	Title and description
<input checked="" type="checkbox"/> F	MECHANICAL ENGINEERING; LIGHTING; HEATING; WEAPONS; BLASTING ENGINEERING IN GENERAL
<input checked="" type="checkbox"/> F16	ENGINEERING ELEMENTS AND UNITS; GENERAL MEASURES FOR PRODUCING AND MAINTAINING EFFECTIVE FUNCTIONING OF MACHINES OR INSTALLATIONS; THERMAL INSULATION IN GENERAL
<input checked="" type="checkbox"/> F16H	GEARING
<input checked="" type="checkbox"/> F16H 2200/00	Transmissions for multiple ratios
<input checked="" type="checkbox"/> F16H 2200/20	• Transmissions using gears with orbital motion
<input checked="" type="checkbox"/> F16H 2200/2002	•• characterised by the number of sets of orbital gears
<input checked="" type="checkbox"/> F16H 2200/2005	••• with one sets of orbital gears

Fig. 15 Classification Research for Planetary Transmission [16]



2.3.3. KR101971189B1 , Transmission of Electric Vehicle

The patent is assigned by Valeo Kapec Co.,Ltd.

The invention comprises a planetary gasket transmission. It includes planetary gasket elements sun gear, ring(annulus) gear, planet (pinion) gears and a carrier (spider). The motor through an input shaft is connected to the sun gear. The gear reduction is provided by the stationary ring and the carrier is the output.

This is a two-speed gearbox. There are two electromagnets, one of them is between the ring and the casing, which makes the ring stationary when engaged and the planetary gasket works as a reductor. The second electromagnet is between the ring and the carrier, which makes the planetary gasket working as a direct drive when engaged. There cannot be any free rotation of the ring. Otherwise the planetary gasket become a differential with two degrees of freedom and no power will be transmitted.

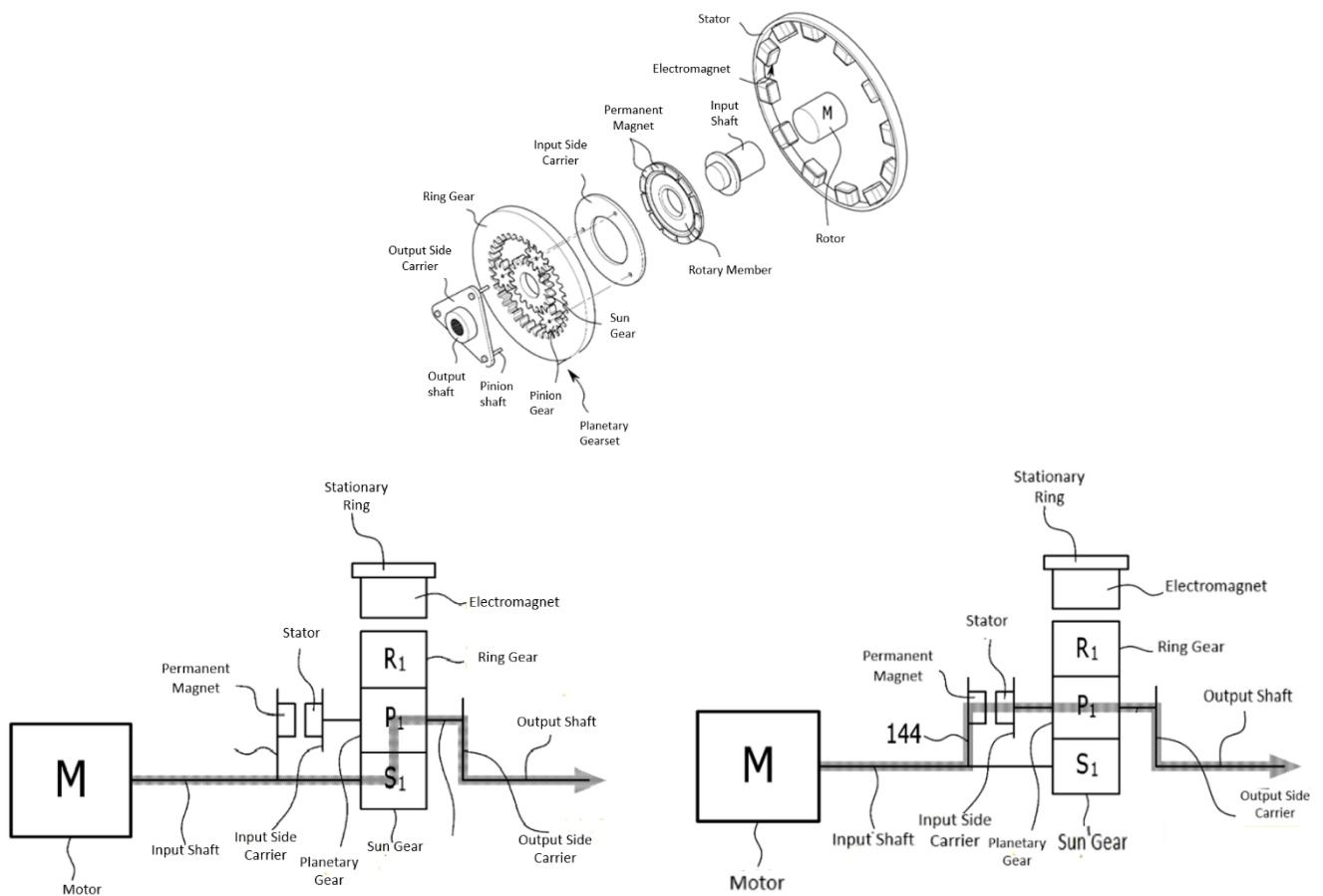


Fig. 16 The Patented Transmission For Electric Vehicle and Power Flow[17]



2.3.4. WO2019214995A1 , Multi-speed Planetary Transmission

This patent is assigned by Robert Bosch GmbH.

This invention consists of a drive shaft, planetary gearset, a clutch which provides a connection between input and output shaft, a freewheel and a locking element which is a dog clutch. In this multi speed planetary gearset the speed shift is done by the clutch engagement .

When the first gear is engaged the ring gear is blocked, and the clutch is not applied, as a result speed of the input shaft reduced. When the second gear engaged, the clutch is applied, and the ring gear is released as a result all the planetary gearset parts rotate together and create a high-speed output.

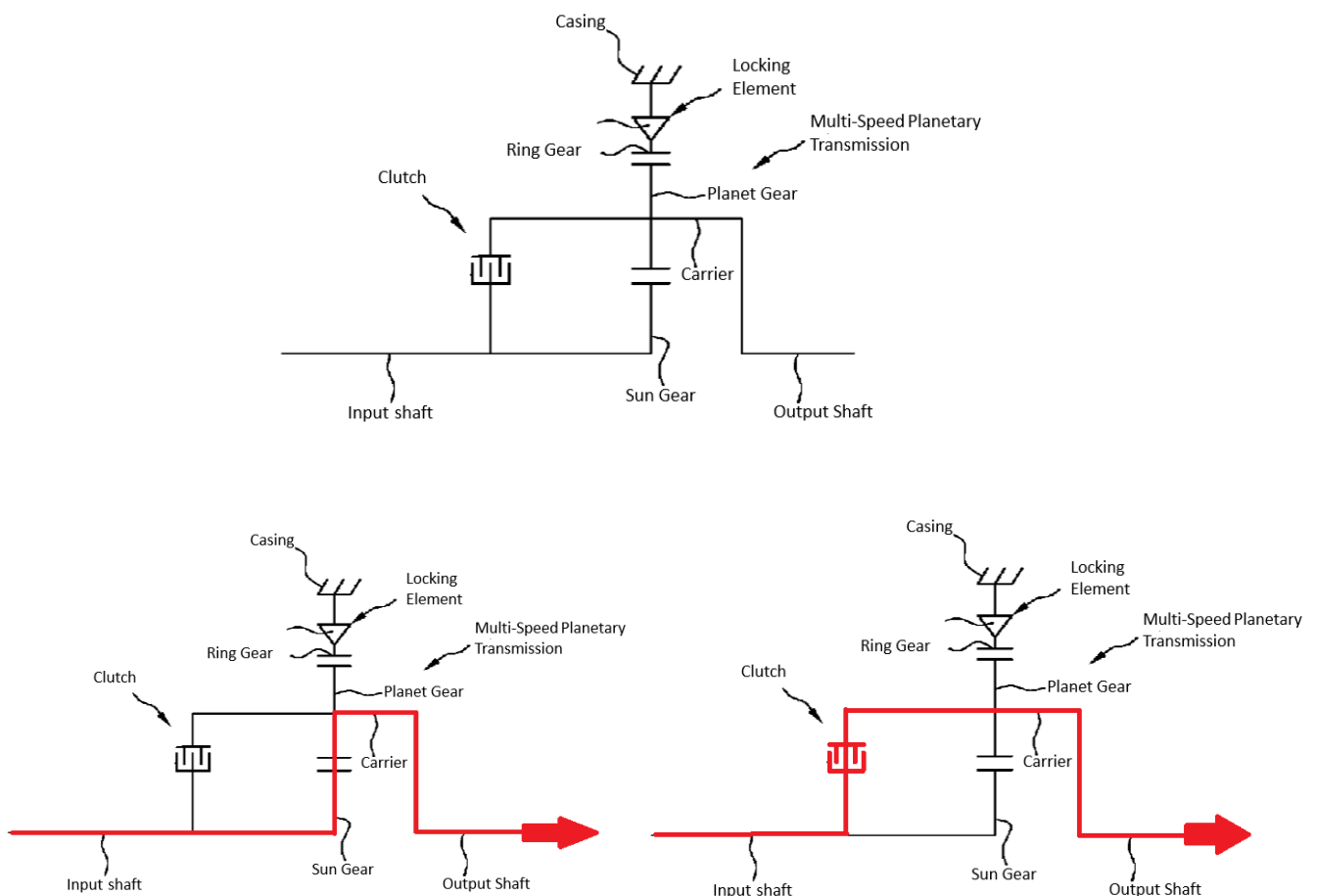


Fig. 17 Multi Speed Planetary Transmission for Vehicle and Power Flow [18]



2.3.5. WO2019115204A1, Electric Drive for a Motor Vehicle

The patent is assigned by Daimler AG.

This invention consists of an electric vehicle, a planetary gearbox includes two planetary sets, a braking element, a clutch and a differential. For the first planetary gearset, sun gear is input, and carrier is output, the ring gear is fixed. For the second planetary gearset the ring(annulus) is input and carrier of the second set is output.

When the first speed is shifted, braking element is activated and the sun gear in the second planetary gearset is fixed. The power which is coming from the first gearset is directed to ring gear of the second set and from there directed to differential & output shaft. When the second gear is shifted the clutch is applied, the ring and the sun of the second planetary gearset will rotate with the same speed, as a result the power comes from the first planetary gearset is directed to differential & output shaft.

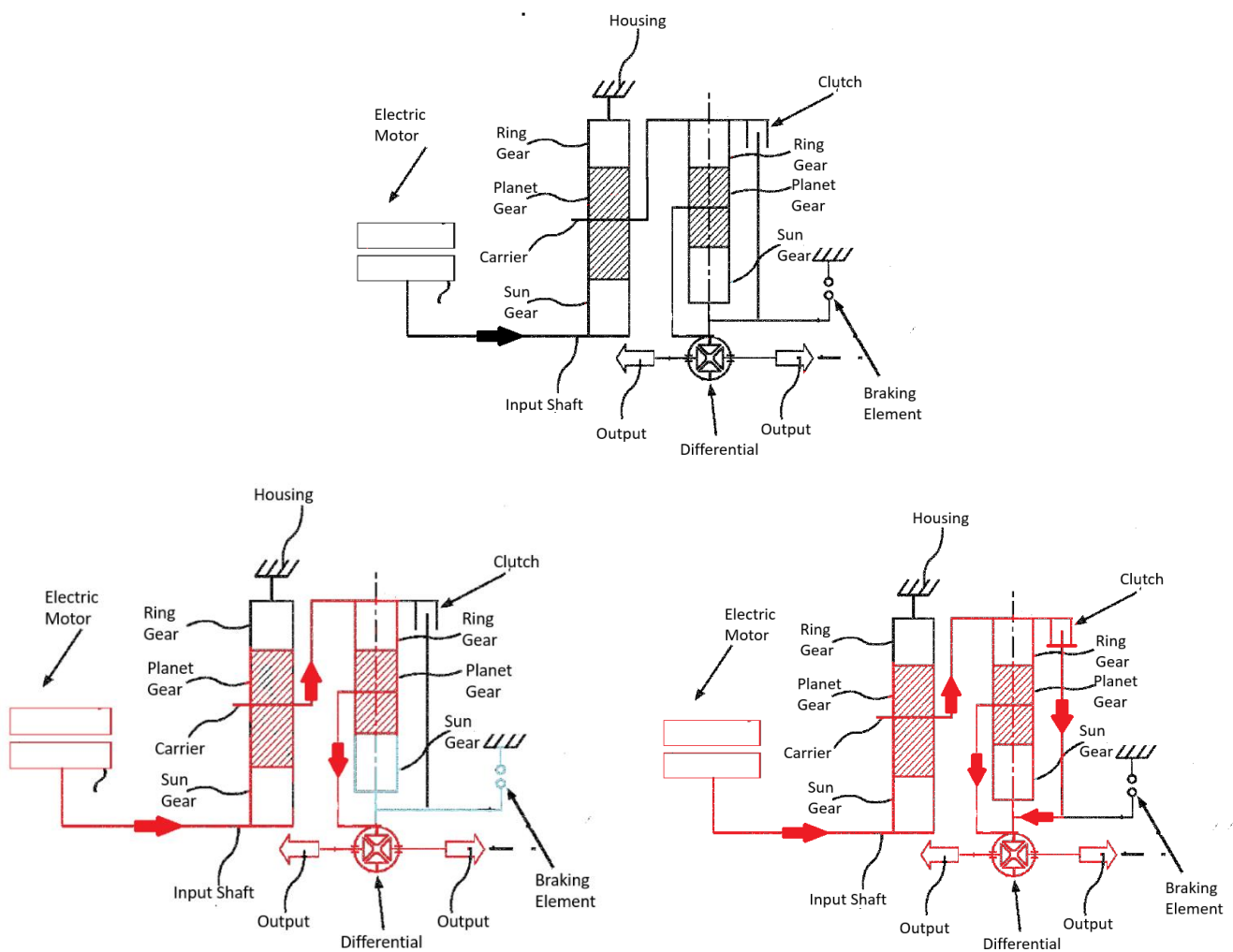


Fig. 18 WO2019115204A1 Patent Design and the Power Flow [19]



2.3.6. WO2019091719A1 , Transmission for an Electric Vehicle

This patent is assigned by ZF Friedrichshafen AG.

The invention includes an electric motor, a dual clutch element, a layshaft transmission system and an oil pump. Oil pump is connected to electric motor, which is always driven regardless from the clutches. When the first clutch (Clutch1) is engaged, the power follows the Shaft1, and there will be a speed reduction in the output shaft. When the second clutch is engaged; the power follows the Shaft2 respectively.

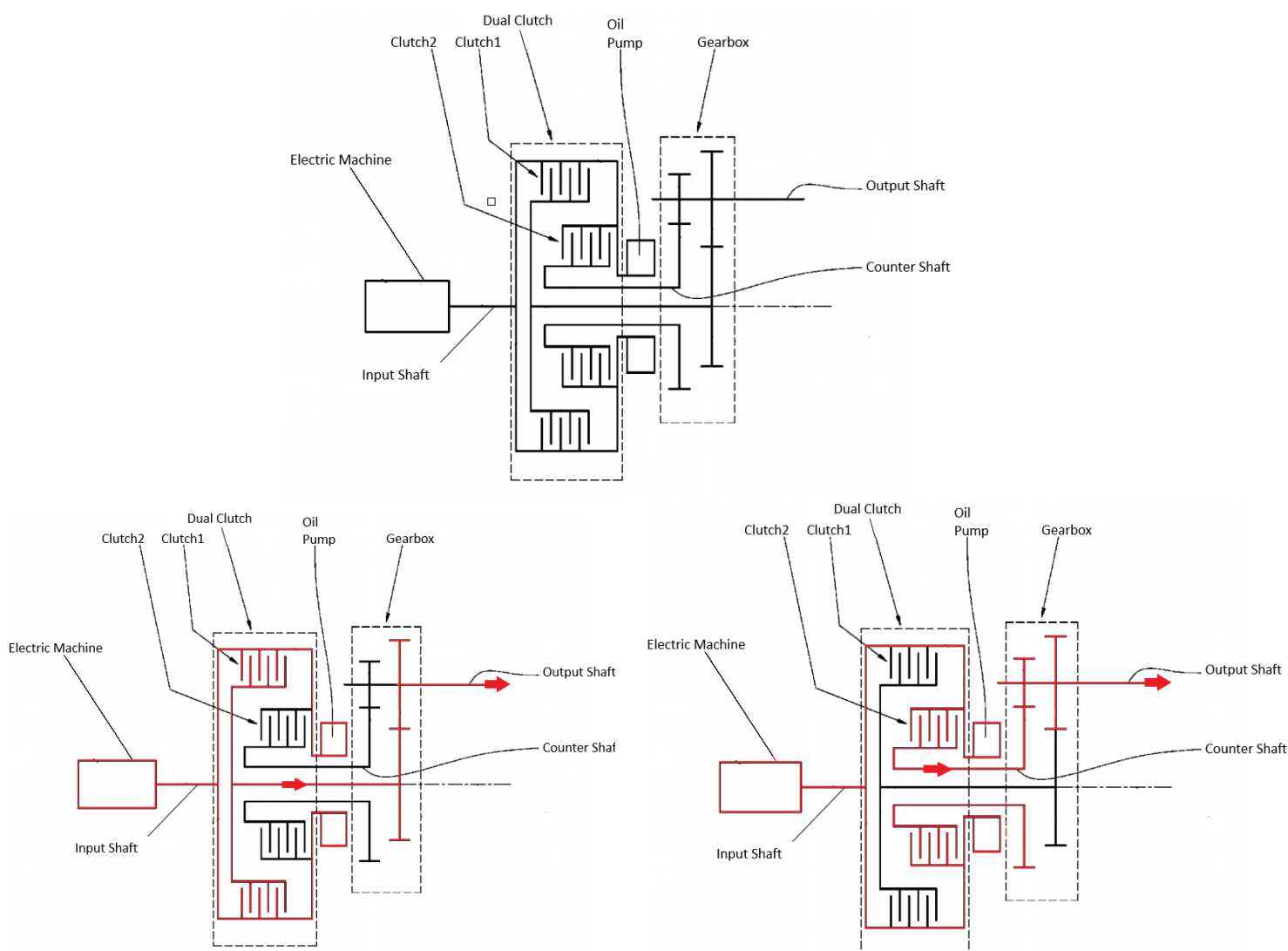


Fig. 19 WO201909179A1 Patent Design and Power Flow [20]



2.3.7. US20160003351A1, Two-Speed Transmission for Vehicle

This patent is assigned by Hyundai Motor Co. Ltd.

The invention includes an electric motor, a planetary gearset which the sun gear is connected to the input and the carrier is connected to the output shaft, clutch elements which is a friction clutch, used in the connection of the sun gear and the carrier and a dog clutch which controls the movement of the ring gear.

When the first speed is engaged, the dog clutch connects the ring gear with the housing and the ring gear is fixed. The friction clutch is not engaged so, there is no connection between the sun gear and the planet carrier. As a result, the power from the motor will be transmitted to sun gear and through the sun gear to the planet carrier respectively and speed is reduced regarding to the gear ratio. When the second gear is engaged the dog, clutch releases the ring gear, the friction clutch create the connection between the carrier and the sun gear. As a result, all of the planetary gear parts will rotate with the same speed and it becomes direct drive.

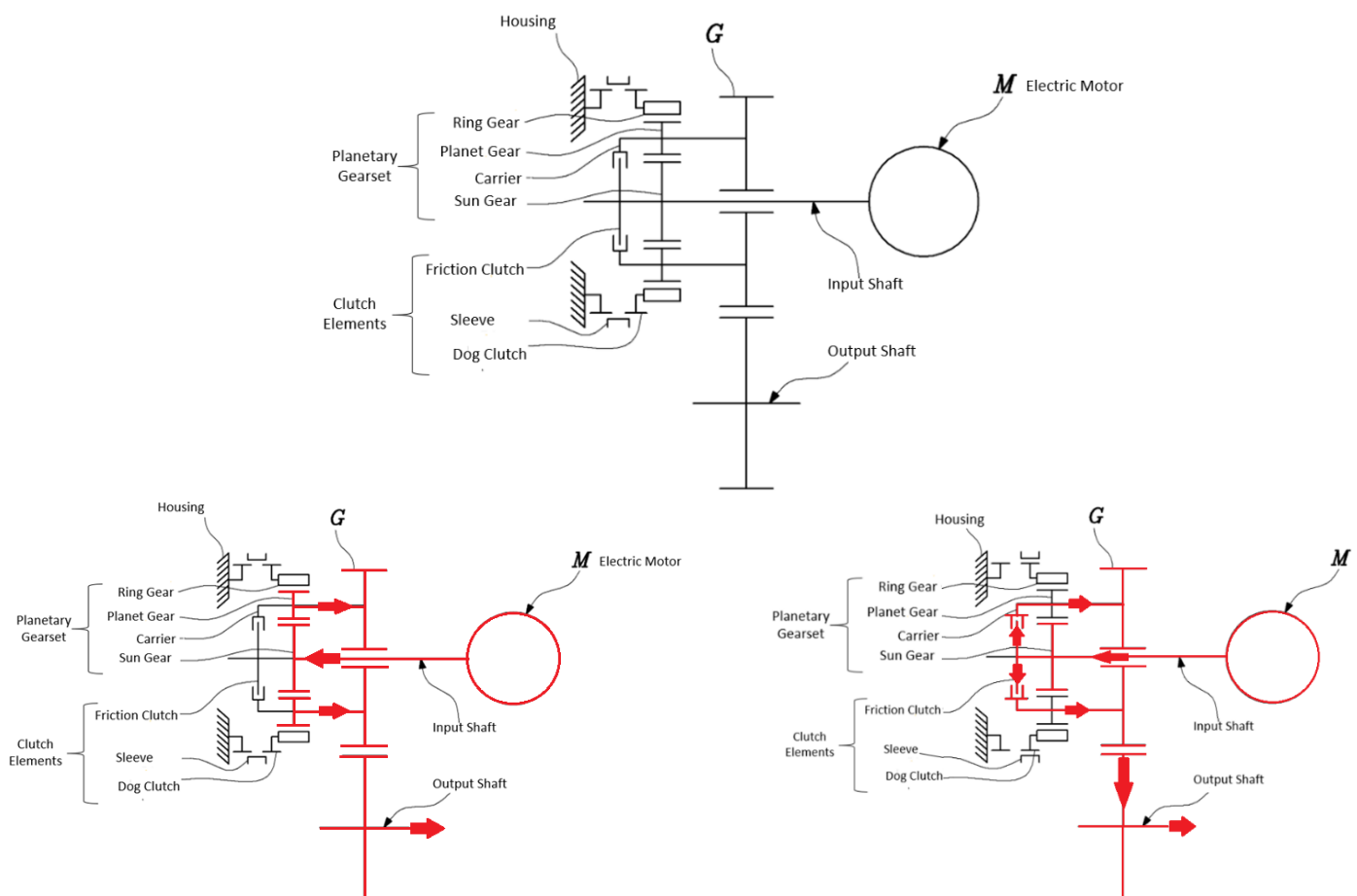


Fig. 20 US20160003351A1 Patent Design and Power Flow [21]



3. Vehicle Parameters and Energy Source Selection

3.1. Parameters of Chevrolet Bolt EV

To start with the design of the vehicle transmission, the most crucial part is determining the parameters of the vehicle and from the data calculating the power requirements of the vehicle. As it can be seen from the current state of art of the vehicles are on the market, the most of them are compact, city car designs. The objective of the thesis is working on a city car which the range of the electric vehicle is adequate for daily urban activities.

From that information the vehicle parameters of the Chevrolet Bolt EV is going to be used for the transmission design.

The specifications are inserted below :

Tab. 2 Specifications of Chevrolet Bolt 2020 [22]

Chevrolet Bolt EV 2020	
Curb Weight (kg)	1616
Width (mm)	1765
Height (mm)	1595



Fig. 21 Chevrolet Bolt 2020 Front View [22]



3.2. Longitudinal Dynamics Calculation

Since the car parameters has been chosen, the longitudinal dynamics properties and the electric motor selection can be done. The main task is to achieve the maximum velocity, which is a required input parameter. So, the maximum velocity is selected as 160 km/h (44.4m/s). With the data of the maximum velocity, the power requirement for the highest speed could be calculated. Driving resistance calculations normally assumed from straight running on horizontal and dry surface.

The traction force required at the drive wheels is called as sum of the acting forces to vehicle.

It is calculated as ;

$$F_{res} = F_r + F_d + F_a + F_{st} \quad \text{Eq. 1}$$

The F_r represents the rolling resistance, F_d represents the air drag, F_a represents the acceleration resistance and F_{st} represents the gradient resistance. Let's have a detailed look in every term in the formulation.

3.2.1. Rolling Resistance

The rolling resistance is calculated by ;

$$F_r = F_N * f = m * g * f * \cos(\alpha) \quad \text{Eq. 2}$$

Where , m is the weight of the vehicle, g is the gravity constant and f is the rolling resistance coefficient. In our calculations the rolling resistance coefficient will be accepted as a constant $f=0.015$ [23].

3.2.2. Air Drag

The air passes through the vehicle in high velocities and creates a drag force.

The air drag is calculated by ;

$$F_d = 0.5 * \rho_{AIR} * C_W * A * v^2 \quad \text{Eq. 3}$$



In this formula ρ is the density of air. At the pressure 1.013 bar with a relative humidity of 60% at 20°C temperature the $\rho_{air} = 1.2 \text{ kg/m}^3$ [23]. "Cw" is the drag coefficient, and the Chevrolet Bolt EV's drag coefficient is $C_w = 0.32$ [24]. A is the cross-sectional area of the vehicle. The recommended value of the cross-sectional area by Ricardo is $A = 1.95 \text{ m}^2$.

3.2.3. Acceleration Resistance

When the vehicle velocity increases or decreases, additional inertia forces take place.

The acceleration resistance is calculated by ;

$$F_a = m * a * \delta \quad \text{Eq. 4}$$

In the formula m represents the weight of the vehicle, a represents the acceleration and the term δ represents the inertial forces of the all rotating masses in the vehicle. The recommended value is provided as $\delta = 1.2$ [25].

3.2.4. Gradient Resistance

When the vehicle is going uphill, the gradient resistance takes place. The gradient resistance acting on the vehicle is calculated by ;

$$F_{st} = m * g * \sin(\alpha) \quad \text{Eq. 5}$$

In the formula m represents the weight of the vehicle, g is the gravitational force and α is the angle of the slope of the road. The acting forces on the vehicle going uphill are represented in the figure, Fig.22.

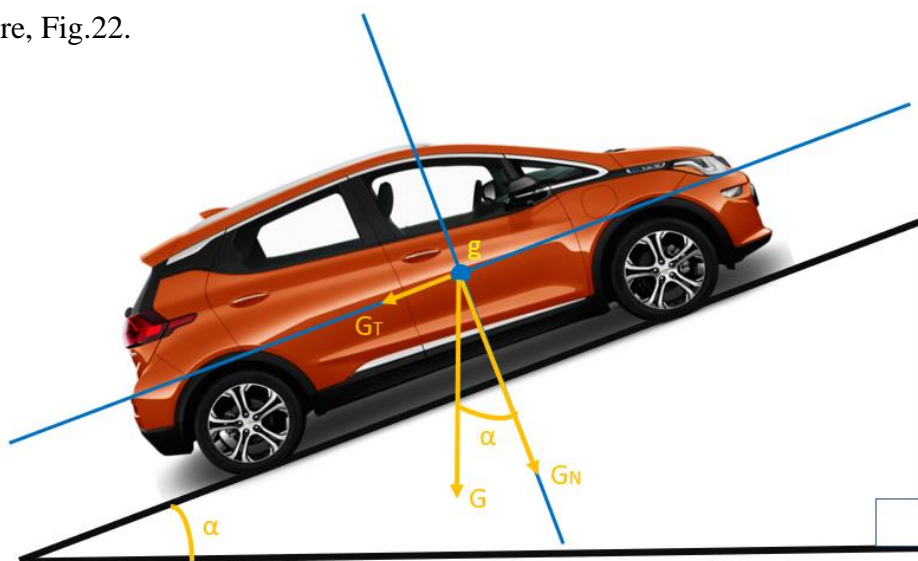


Fig. 22 The Forces Acting on the Vehicle, Uphill Movement



3.3. Total Driving Resistance

In the previous section, the tractive force calculation described in the equation 1.

If the equation would be described in extended version, the equation 1 becomes like ;

$$F_{res} = F_r + F_d + F_a = m * g * f + 0.5 * \rho_{AIR} * C_W * A * v^2 + m * a * \delta$$

Tab. 3 Input Parameters for Calculation of Total Driving Resistance

Curb Weight [22]	m	1616 kg
Weight of Driver	md	70 kg
Coefficient of Rolling Resistance	F	0.015
Drag Coefficient [24]	C _w	0.32
Cross Sectional Area	A	1.95 m ²
Kinematic Radius of Tire	R _d	0.301 m
Efficiency of Driveline	η _t	0.90
Air Density [23]	ρ _{air}	1.2 kg. m ⁻³
Gravitation Constant	g	9.81m.s ⁻²
Inertia of the Rotating Masses	δ	1.2

When the driving resistance for the maximum velocity calculated, since the car is going with maximum speed, there is no acceleration resistance (a= 0). And the formula would be ;

$$F_{res} = F_r + F_d = m * g * f * \cos(\alpha) + 0.5 * \rho_{AIR} * C_W * A * v^2 \quad \text{Eq. 6}$$

$$F_{res} = F_r + F_d = 1686 * 9,81 * 0,015 * 1 + 0,5 * 1.2 * 0,32 * 1,95 * \left(\frac{160}{3.6}\right)^2$$

$$F_{res} = F_r + F_d = 987.6 N$$

The power which is transferred to the wheels is equal to multiplication of resistance forces and velocity. From that equation, the cubic equation of the velocity is obtained with power is the unknown value. With that result, the estimation of the power requirement can be observed, an adequate electric motor can be selected.



The power which is transferred to the wheels is calculated by ;

$$P * \eta t = (Fr + Fd) * v \quad \text{Eq. 7}$$

$$P * \eta t = (m * g * f + 0.5 * \rho_{AIR} * C_W * A * v^2) * v$$

$$P * \eta t = m * g * f * v + 0.5 * \rho_{AIR} * C_W * A * v^3$$

$$P * 0.90 = 1686 * 9.81 * 0.015 * \left(\frac{160}{3.6}\right) + 0.5 * \rho_{AIR} * C_W * A * \left(\frac{160}{3.6}\right)^3$$

$$P = 54635 W = 54.6 kW$$

As a result, the power requirement of the electric motor is approximately 54.6 kW.

With the data calculated, the electric motor selection can be done.

3.3.1. YASA P-400 RS Electric Motor

To be able to make an adequate selection for the electric machine, the required power and torque of the electric machine should be considered. When the market research for the electric motors done the model YASA P-400 RS meets the requirements for the power.

The electric motor P-400 RS provides up to 94% motor efficiency and high maximum speed (up to 8000 rpm) [28].



Fig. 23 YASA P-400 RS PMSM Electric Motor [26]



The specifications of the YASA P-400 RS are listed below :

Tab. 4 YASA P-400 RS Specifications

Mechanical		Electrical	
Casing Diameter	305mm	Peak Torque	Up to 370 Nm
Axial length	106.7mm	Continuous Torque	Up to 200 Nm
Dry Mass	28.2 kg	Continuous Power	Up to 60 kW
Stator Cooling	Oil	Maximum Speed	8000 rpm
Mounting	294mm PCD	Peak Power	160kW

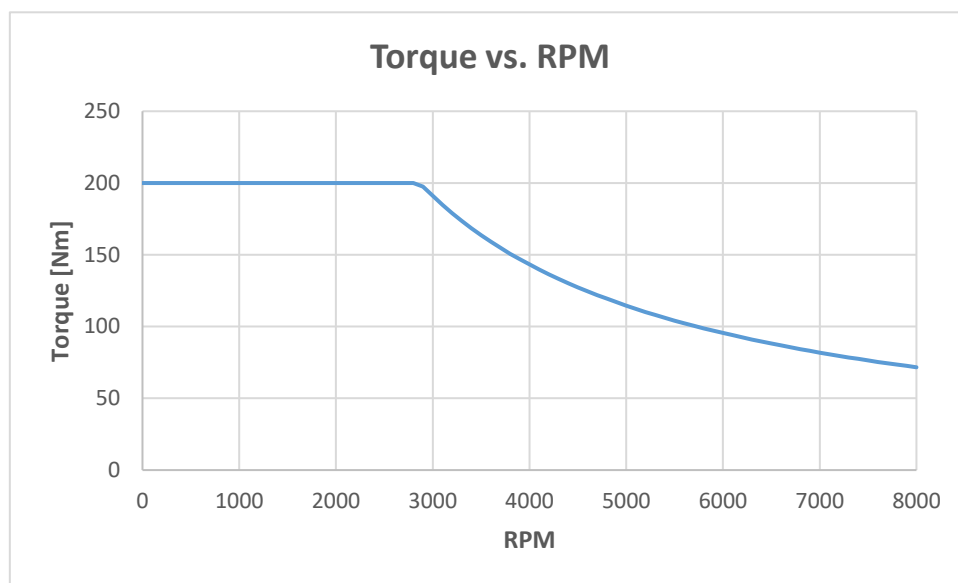


Fig. 24 The Chosen YASA Motor Characteristics

To get the tractive force on the wheels the following formula is used;

$$F_{tr} = \frac{M_e * i * \eta_{tr}}{r_d} \quad \text{Eq. 8}$$

In this formula M_e represents the torque of the electric motor, i is the gear reduction ratio, η_{tr} is the efficiency of the transmission system and r_d is the dynamic radius of the vehicle. The only unknown value here in the equation 8 is the gear reduction ratio i , and it can be found from the maximum velocity of the vehicle (160km/h=44.4m/s).



The gear reduction ratio (i) is calculated in the condition of the maximum speed. So, the equation of the maximum speed at the engine is ;

$$V_{max} = \omega * rd = \frac{2 * \pi * n}{60} * \frac{rd}{i} \quad \text{Eq. 9}$$

In this equation n is the velocity of the motor in rpm , ω is the angular velocity of the motor in s-1, rd is the dynamic radius of the vehicle. Traction Limit Due to Tire Adhesion

If the equation would be converted for finding the gear reduction ratio i , it becomes ;

$$i = \frac{2 * \pi * n}{60} * \frac{rd}{v} \quad \text{Eq. 10}$$

$$i = \frac{2 * \pi * 8000}{60} * \frac{0.301}{44.44}$$

$$i = 5.6737$$

The resulting final ratio is equals to $i=5.6737$.

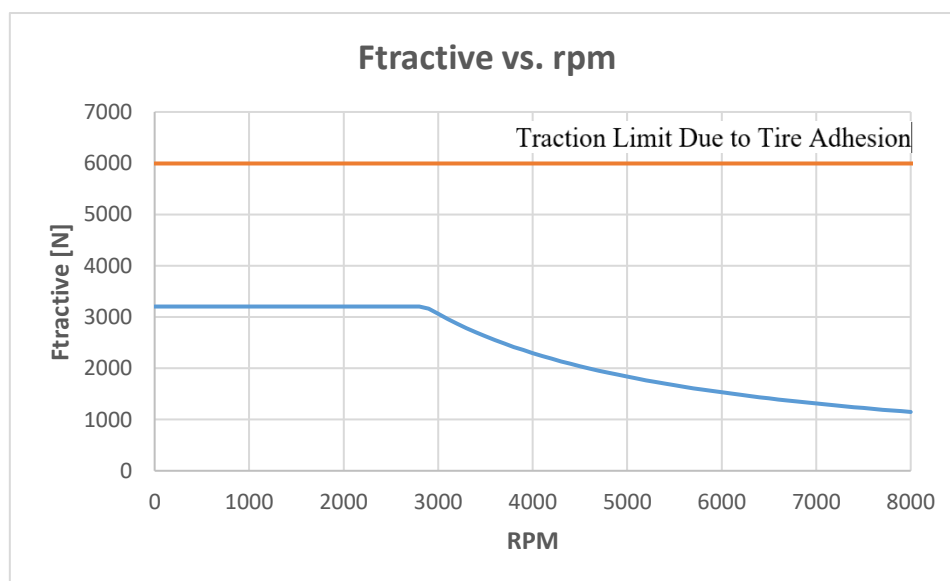


Fig. 25 Tractive Force vs. RPM



From the vehicle parameters given, in the enclosed Microsoft Excel file ;
Torque, Resistance Forces, Tractive Forces, distance taken have been calculated, and from the results the graphs have obtained. These graphs are ;

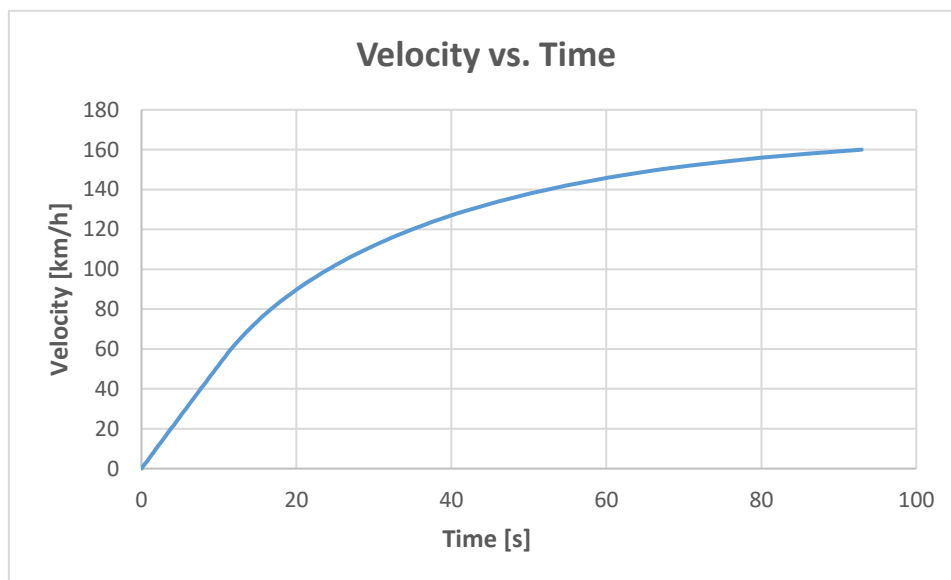


Fig. 26 Velocity vs. Time

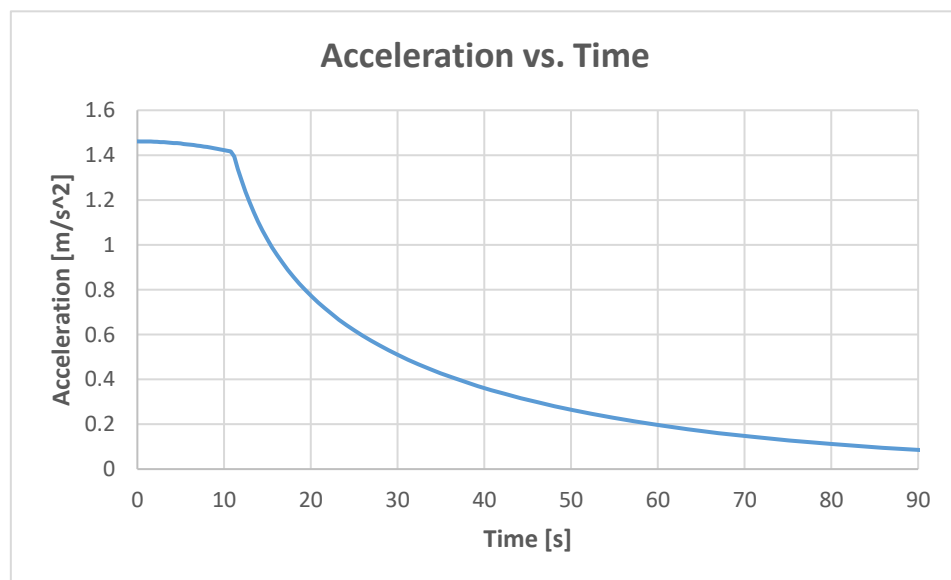


Fig. 27 Acceleration vs. Time

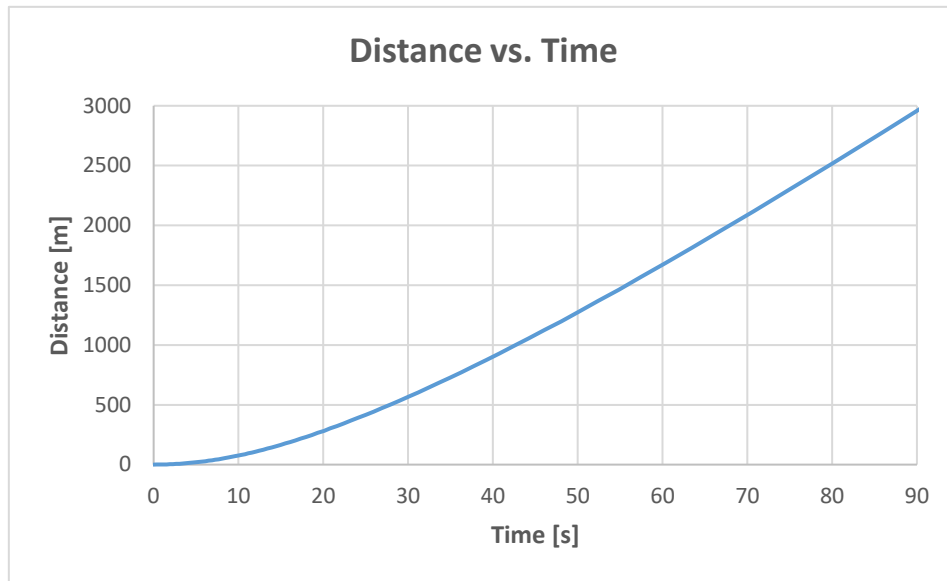


Fig. 28 Distance vs. Time

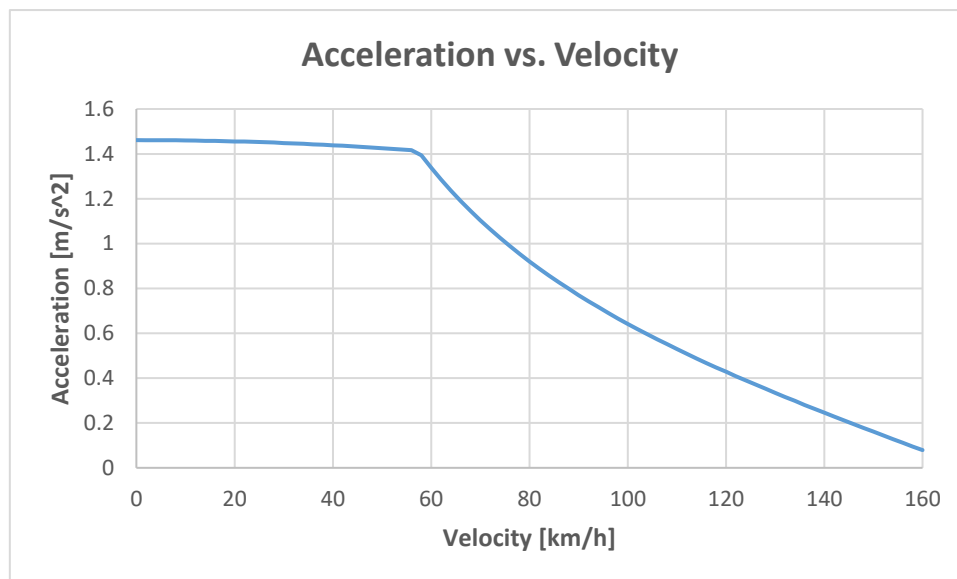


Fig. 29 Acceleration vs. Velocity

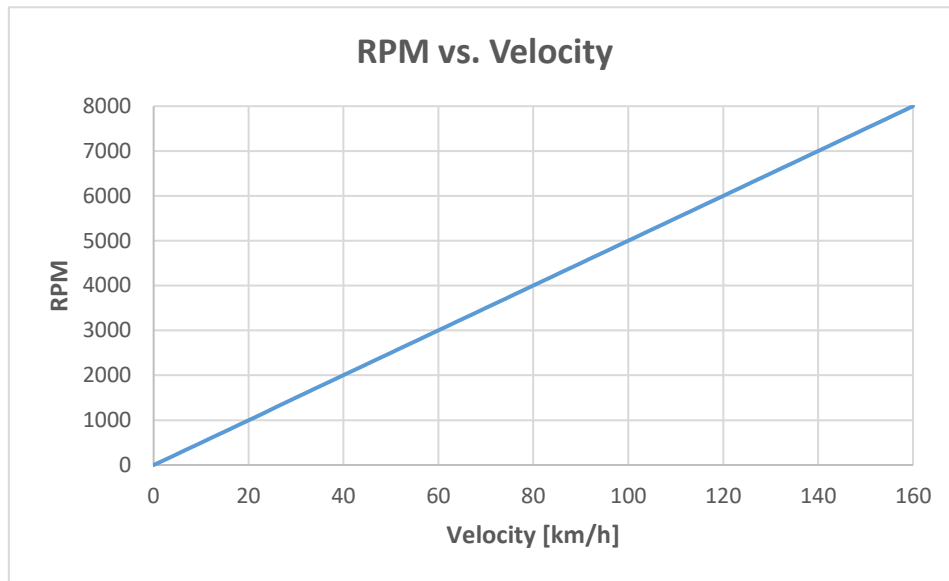


Fig. 30 RPM vs. Velocity

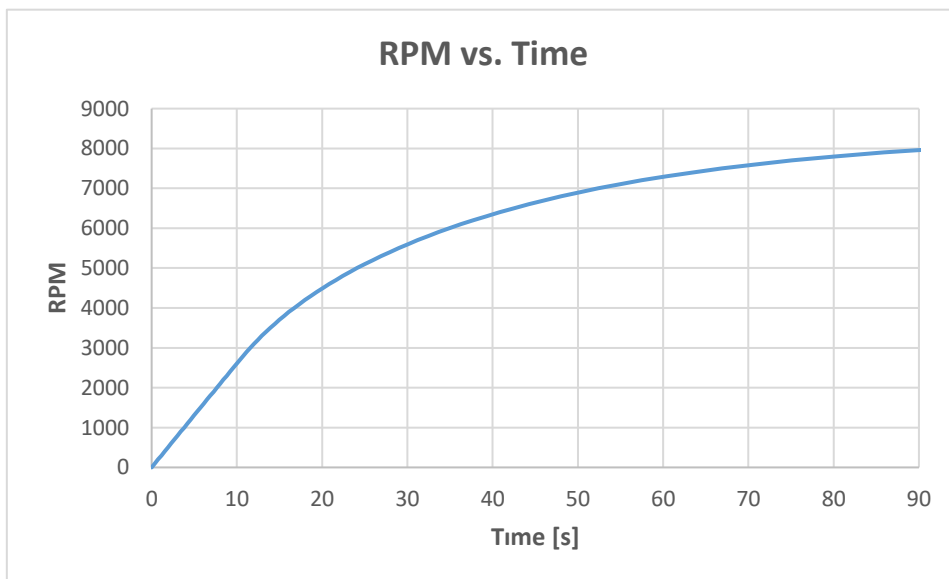
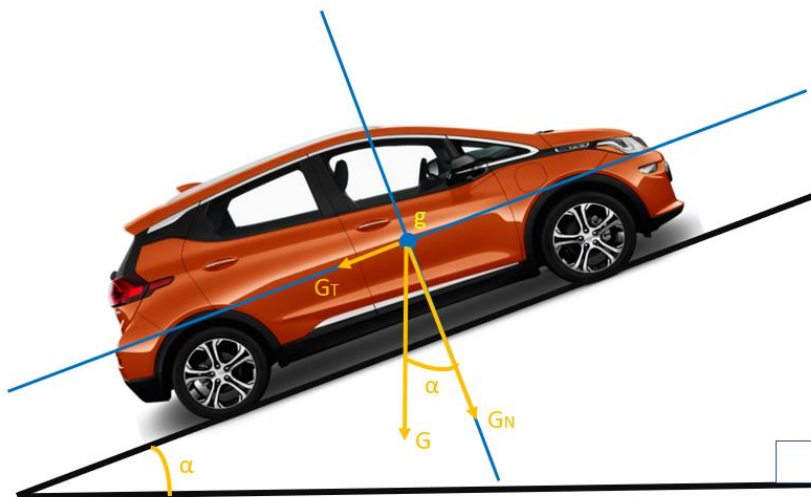


Fig. 31 RPM vs. Time



Also, we would like to know the how many percentages of slope our car could climb maximally.

To be able to calculate that, let's assume there are four passengers which is $m_{pass}=280\text{kg}$ and $m_{cargo}=50\text{kg}$, which is $m_{payload} = 330 \text{ kg}$ in total.



m_{curb}	1616 kg
m_{pass}	280 kg
m_{cargo}	50 kg
m_{total}	1946 kg

To be able to find the maximum slope the car could climb uphill, we need to know the maximum torque which the electric motor can provide continuously, which can be found from the following equation ;

$$F_w = \frac{M_e * i}{r_d} \quad \text{Eq. 11}$$

$$F_w = \frac{200\text{N} * 5.6737}{0.301}$$

The electric motor can provide maximum 1134.74 Nm that, the maximum resistance force which is applied to tires must not be exceed 3769.918 Newtons. The assumption is, the vehicle is in the beginning of the slope and just going upwards, and as a result the drag and acceleration resistance are taken as zero($F_d=0$, $F_a=0$).



The resistance forces applied to vehicle while going uphill;

$$F_{res} = F_r + F_{st} \quad \text{Eq.12}$$

$$F_{res} = m * g * f + m * g * \sin(\alpha)$$

$$3769.918 = 1946 * 9.81 * 0.015 + 1946 * 9.81 * \sin(\alpha)$$

$$\sin(\alpha) = 0.18247$$

$$\alpha = 10.51^\circ$$

The maximum slope the car could climb uphill would be found as 10.51° and if it would be converted into a tangent slope in % ;

$$\tan(10.51) = 0.185 = 18.5\%$$

The vehicle could go up **maximum 18.5% slope** without a problem.



4. Efficiency, Mass and Dimension Comparison of the Transmission Systems

In the previous chapters, the transmission systems of the automobiles currently available on the market and the existing patent solutions were discussed. To proceed further, from the solutions three variants will be selected and their efficiency, mass and dimension comparison will be addressed.

The first variant of the transmission system is Audi e-tron's design ; planetary reduction with additional simple parallel gear step to differential.

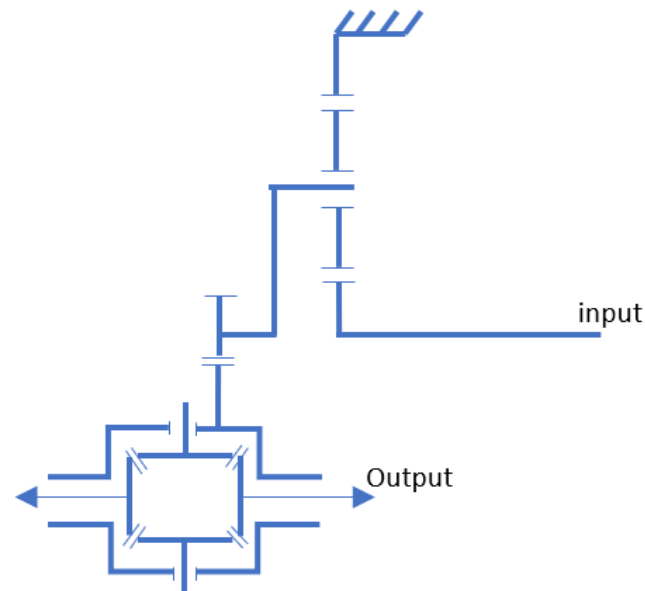


Fig. 32 Planetary Reduction With Additional Simple Parallel Gear Step



Second variant of the transmission system is the common layshaft transmission design which are used in many cars: Two stage parallel shaft with compound gears on the layshaft in the Figure 33.

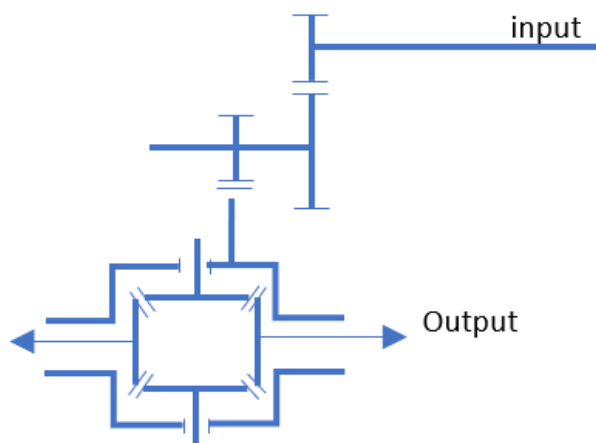


Fig. 33 Two Stage Parallel Shaft, Layshaft Transmission

The third variant of the transmission system is planetary gear reductor with compound planets, used in Jaguar I-Pace. In this design as mentioned, there are two gear meshes, in the first mesh, there is no ring gear and the planet of the first mesh is compound with the second planet.

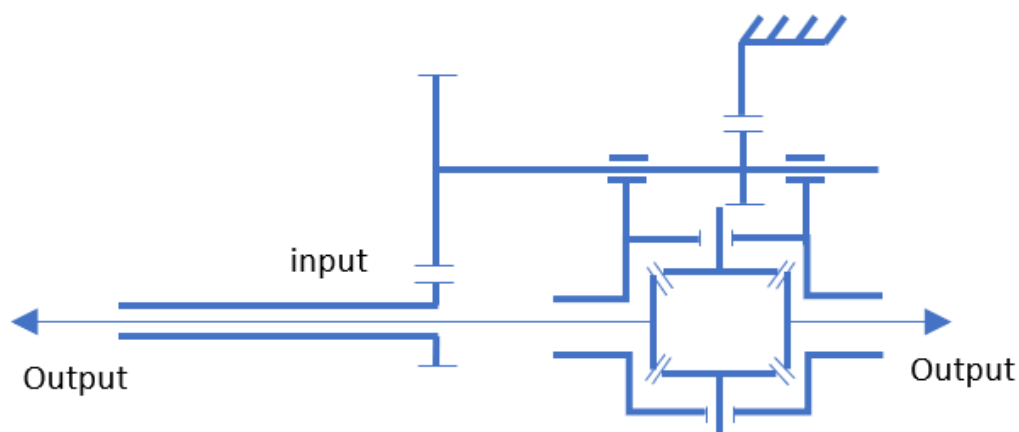


Fig. 34 Planetary gear reductor with Compound Planets



4.1. Efficiency and Losses

There is no device in the world which is working with 100% efficiency. This situation is also valid for the transmission systems. There are several losses taken into account when the transmissions are running. The efficiency is not constant due to unavoidable losses, and due to increase of the rotational speed, temperature of the oil, viscosity of the oil and temperature changes and it cause a decrease in output torque[27]. In this chapter all the losses in the efficiency are undertaken.

4.1.1. Lubrication Losses

In the current state of art automotive transmissions the oil splash system is being used. Since their effect on the losses can not be calculated analytically, by the help of experimentation method the lubrication losses are found. In the ordinary conditions, the lubrication losses are less than 1%. ($\zeta_{\text{losses}} < 1\%$) [28]. But, to be able to estimate their numerical value, the lubrication losses will be accepted as $\zeta_{\text{losses}} = 1\%$. This approximation is going to be used in all variants of the transmissions calculation.

4.1.2. Meshing (Tooth-Friction) Losses

The meshing losses are the most important part of the losses. The accuracy of the efficiency losses in meshings are difficult but engineers could provide some equation for their calculation. The approximate efficiency losses for helical gears are calculated as ;

$$\zeta_{\text{helical}} = \frac{f * \pi * \varepsilon}{4 * \cos \beta} * \left(\frac{1}{Z_p} \pm \frac{1}{Z_g} \right) \quad \text{Eq. 13}$$

In this equation f represents the coefficient of friction, ε represents transverse contact ratio and β represents the helix angle. Instead of making this long calculation, there is a table described in Mrs. Achtenova's book [29]. For simplification the mean value of the range of the table are going to be used.

Tab. 5 Reference Values of Meshing Friction Losses [29]

Type of Gear	Range of Coefficient of losses	Coefficient of losses used
Spur or Helical Gears (External Gears)	0.015-0.025	0.02
Annular Gears (Spur or Helical)	0.005-0.015	0.01
Bevel Gears	0.02-0.03	0.025
Hypoid Gears	0.025-0.04	0.03



4.1.3. Losses in Bearings

The power loss in the bearings is calculated from the formula;

$$|P_{\zeta_{bearing}}| = |M_{\zeta}| * \omega_P \quad \text{Eq. 14}$$

$$|M_{\zeta}| = F * f * r_m \quad \text{Eq. 15}$$

In these equations, M_{ζ} represents frictional torque, F is the load of bearing and f is the coefficient of friction and r_m is the main radius on which the elements are rolling. Also for simplification of the estimation and since there is no numbers for calculation, Ricardo suggests that, each shaft requires an existence of two bearings and each bearing cause approximately 1% lose in the efficiency.

The components which are supposed to be the same in all considered variants are not described in the table(differentials, half shafts etc.).

With those approximations, let's analyse all three variants ;

Variant 1 ;

Planetary reduction with additional simple parallel gear step to differential.

Since it is a planetary gearbox the efficiency calculation is done by the Willis formulas and the torque equilibrium in the system.

In this variant the number of teeth of the ring gear is $Z_R = 108$, and number of teeth of the sun gear is $Z_S = 69$.

The basic ratio is found as;

$$i_{\text{Basic}} = \frac{Z_R}{Z_S} = \frac{108}{69} = 1.565 \quad \text{Eq. 16}$$

$$i_{PGS} = 1 + i_{\text{Basic}} = 2.565 \quad \text{Eq. 17}$$



With the internal and external meshes the efficiency coefficient is ;

$$\eta = 1 - 0.2 - 0.1 = 0.97 \quad \text{Eq. 18}$$

Willis formulas provides the speed equation ;

$$n_S - \left(1 + \frac{z_R}{z_S}\right) * n_c + \frac{z_R}{z_S} * n_R = 0 \quad \text{Eq. 19}$$

In the equation n_S represents the speed of the sun , n_c represents the speed of the carrier and n_R represents the speed of the ring . It is known that the variant one has stationary ring, so the $n_R = 0$. And the sun gear speed is equal to the speed of the electric motor.

The torque equilibrium represents;

$$T_s + T_R + T_c = 0 \quad \text{Eq. 20}$$

Without Loses ;

$$\frac{z_R}{z_S} * T_S - T_R = 0 \quad \text{Eq. 21}$$

With Losses ;

$$\frac{z_R}{z_S} * \eta^{Sign(P_S)} * T_S - T_R = 0 \quad \text{Eq. 22}$$

Powers are calculated by the multiplication of the torques and the rotational speeds ;

$$P = T * n \quad \text{Eq. 23}$$



With the matrix method the relative speeds of the all rotating elements and their powers with and without losses can be found;

		PG ratio = 2.56522							
zS/zR	1.56522								
Eta	0.97								
		nS	nC	nR					
Willis formula		1	-2.5652	1.56522	0	nS =	1		
fixed Ring		0	0	1	0	nC =	0.38983		
Sun is input		1	0	0	1	nR =	0		
Without Losses		TS	TC	TR					
Torque relationship		1.56522	0	-1	0	TS =	1	PS =	1
Torque equilibrium		1	1	1	0	TC =	-2.5652	PC =	-1
Torque input		1	0	0	1	TR =	1.56522	PR =	0
With Losses		TS	TC	TR					
Torque relationship		1.51826	0	-1	0	TS =	1	PS =	1
Torque equilibrium		1	1	1	0	TC =	-2.5183	PC =	-0.9817
Torque input		1	0	0	1	TR =	1.51826	PR =	0

Fig. 35 Efficiency Calculation of The Variant One

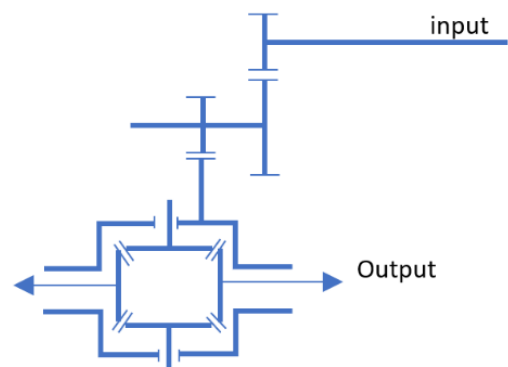
As it can be seen from the Figure 35, since the input efficiency is 100%, the 98.17% of the power can be provided from the output. The amount of the loss is approximately 2% in the planetary gear set.

Variant 2 :

Two stage parallel shaft with compound gears on the layshaft.

The transmission has ;

- Input shaft : 2 bearings = **2%**
- Counter Shaft : 2 bearings = **2%**
- 2 external meshes = **4%**
- Churning of the oil = **1%**



As a result with the simplified efficiency estimation total loss would be 9% and total efficiency would be 91%.



Variant 3 :

Planetary gear reductor with compound planets.

With the matrix method, the relative speeds of the all rotating elements and their powers with and without losses can be found (the same method applied to the variant 1) ;

		PG ratio : 5.54087								
zS/zPS*zPR/zR	4.54087									
Eta	0.97									
		nS	nC	nR						
Willis formula		1	-5.5409	4.54087	0	nS =	1			
fixed Ring		0	0	1	0	nC =	0.18048			
Sun is input		1	0	0	1	nR =	0			
Without Losses		TS	TC	TR						
Torque relationship		4.5409	0	-1	0	TS =	1	PS =	1	
Torque equilibrium		1	1	1	0	TC =	-5.5409	PC =	-1	
Torque input		1	0	0	1	TR =	4.54087	PR =	0	
with losses		TS	TC	TR						
Torque relationship		4.4046	0	-1	0	TS =	1	PS =	1	
Torque equilibrium		1	1	1	0	TC =	-5.4046	PC =	-0.9754	
Torque input		1	0	0	1	TR =	4.40464	PR =	0	

Fig. 36 Efficiency Calculation of the Variant Three

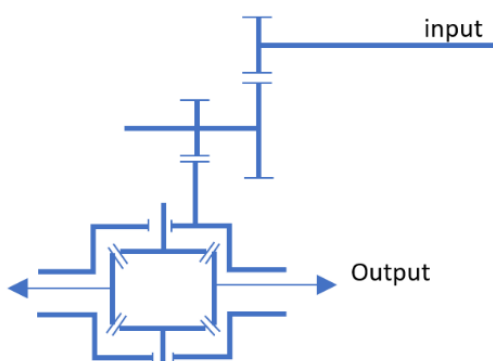
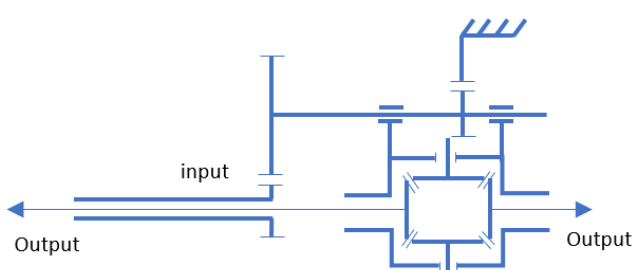
As it can be seen from the Figure 36, since the input efficiency is 100%, the 97.54% of the power can be provided from the output. The amount of the loss is approximately 2.46%. In the planetary gear set.

Tab. 6 Efficiency Estimation of the Variant 1

Variant 1 :	
	<ul style="list-style-type: none"> • Input shaft : 2 bearings = 2% • Carrier Shaft : 2 bearings = 2% • The loss in the Planetary Gearbox ≈2% • External Mesh of Final Drive=2% • Churning of the oil : 1%
	<p>TOTAL LOSS : 9% TOTAL EFFICIENCY : 91%</p>



Tab. 7 Efficiency Estimations of Variant 2 and 3

<p>Variant 2 :</p> 	<ul style="list-style-type: none"> • Input shaft : 2 bearings = 2% • Counter Shaft : 2 bearings = 2% • 2 external meshes = 4% • Churning of the oil = 1%
<p>Variant 3 :</p> 	<ul style="list-style-type: none"> • Input shaft : 2 bearings = 2% • The loss in the Planetary Gearbox \approx 2.5% • Churning of the oil = 1%
	<p>TOTAL LOSS : 5.5% TOTAL EFFICIENCY : 94.5%</p>

As it can be seen from Tables 6 and 7, it is expected that the third variant is more efficient than the first and the second variants.

$$\eta_{VARIANT\ 3} > \eta_{VARIANT\ 1} > \eta_{VARIANT\ 2}$$



4.2. Mass and Dimension Estimation

Since there are no parameters are known with the powertrains the mass estimation will be done by comparing the number of parts in the transmission system and the comparison will be prepared.

For the dimension comparison, it will be done from the transmission's cross sectional drawings and by that their dimensions will be estimated.

4.2.1. Mass Comparison of the Selected Transmission Systems

The first variant; planetary reduction with simple parallel gear step consists of :

- Differential
- Input Shaft
- One set of planet system
- Electric Motor (YASA P 400-RS)
- One parallel gear step (two gear system)
- Half shafts
- Medium Size Medium Weight Casing

The second variant ; two stage parallel shaft, layshaft transmission consists of :

- Differential
- An input shaft with one gear system
- A counter shaft with two gear system
- Electric Motor (YASA P 400-RS)
- Half Shafts
- Large Heavy Casing

The third variant ; Planetary gear reductor with Compound Planets consists of

- An hollow input shaft
- Differential
- First planetary reduction system without ring gear
- Second planetary reduction set without sun gear
- Half Shafts
- Electric Motor (YASA P 400-RS)
- Small Light Compact Casing



It can be seen that with the given variants the differential and the electric motor and half shafts exist on all variants and their effects on the mass are the same.

The first variant has a single set of planetary gear with an input shaft, one set of planetary system and one parallel gear step and a medium size medium weight casing which is different from the other variants.

The second variant has an input shaft with one gear pair and a counter shaft with two gear pairs with a large and heavy casing. .

The third variant has a hollow input shaft, the first planetary gear set without a ring gear and a second planetary reduction set without a sun gear and a small, light and compact casing.

It is expected that the second variant is heavier than the first variant and the third variant is the lightest.

$$m_{\text{VARIANT 2}} > m_{\text{VARIANT 1}} > m_{\text{VARIANT 3}}$$

4.2.2. Dimension Comparison of the Selected Transmission Systems

To be able to make a dimension comparison of the selected comparison systems, the configuration of the systems must be known.

The first variant is planetary single speed reduction. Sun is input, carrier is output, ring is stationary. There is an additional simple parallel gear step to the differential. It is assumed that the length of the transmission system is A, which can be seen in Figure 35.

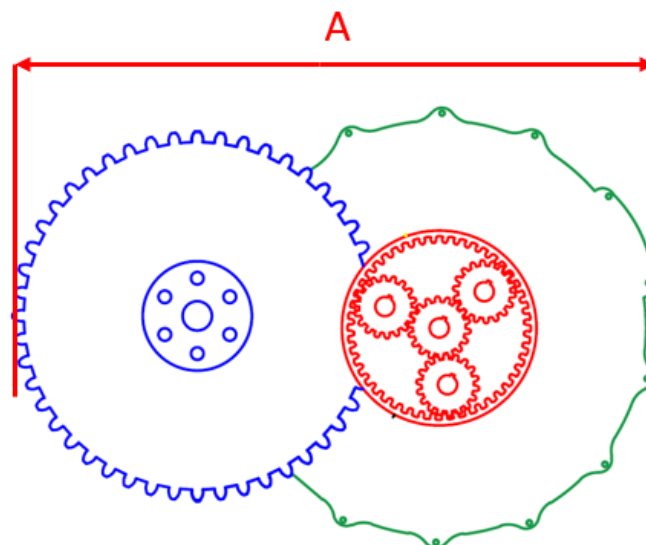


Fig. 37 Configuration of the First Variant of the Selected Transmissions



The second variant is two stage parallel shaft with compound gears on the layshaft.

It is assumed that the length of the transmission system is B, which can be seen in the Figure 36.

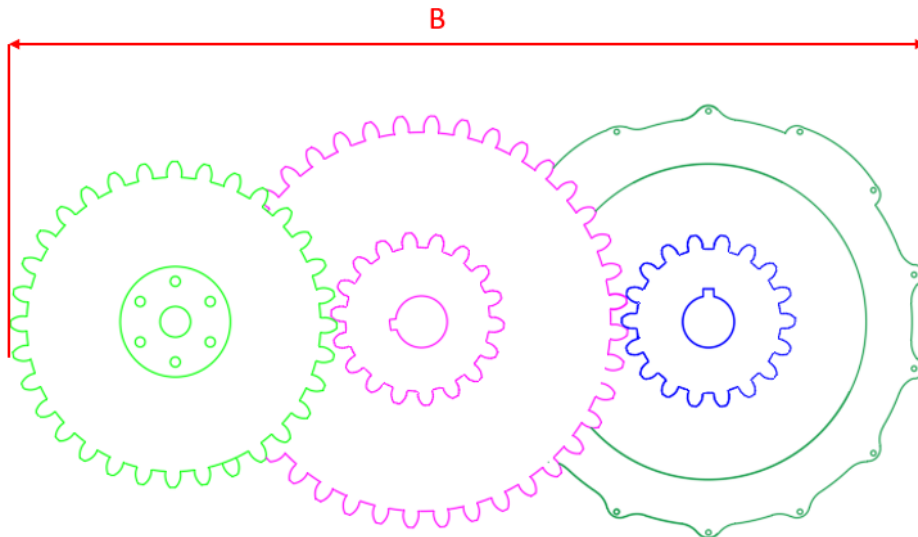


Fig. 38 Configuration of the Second Variant of the Selected Transmissions

The third variant is Planetary gear redactor with compound planets. Sun is input, carrier is output, ring is stationary. Sun is meshing with bigger planet and ring is meshing with smaller planets. It is assumed that the length of the transmission system is C, which can be seen in Figure 37.

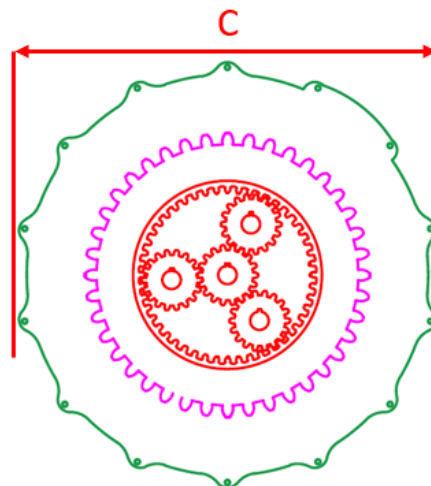


Fig. 39 Configuration of the Third Variant of the Selected Transmissions

As a result, in dimensional point of view, it is expected that length A is larger than length C and smaller than length A. In other words, the second variant occupy more space than the variant two and variant one, respectively.

$$d_{VARIANT\ 2} > d_{VARIANT\ 1} > d_{VARIANT\ 3}$$



5. The Planetary Gearset Design

In the previous chapters, the designs used in the vehicles on the market, patents and solutions have been discussed, the car have been selected and from the given vehicle parameters, resistances and the total ratio requirement have been calculated.

In this chapter, for the requirement of the design, the diameters of the parts, number of teeth of each element, the requirement of the assembly will be discussed. Also with the help of the Ricardo's engineering softwares SABR/GEAR, the duty cycle analysis will be done and the stresses which are affecting the gears during operation and their values will be calculated and the results will be discussed.

5.1. Selection : Planetary Single Speed Reduction

In the previous chapter, since there are more efficient alternatives are exist instead of the selected gearbox for calculation, the requirement for this thesis to work on a design of a planetary gearset, not a layshaft transmission.

Also, if the design variants number one and three are compared, it can be seen the variant three transmission, only the transmission extracted from the powertrain seems more efficient than the selected variant. However, the drivetrain including the homokinetic joints at variant three might be subject of high loses and premature wear. Because the ground clearance in our application have to be gapped and only way to keep the ground clearance with variant three, is keeping the halfshafts highly misaligned.

Variant three is a coaxial design. In order to keep the axes from the differential towards from one of the wheels the rotor of the electric motor should be hollow. It requires a modification in the YASA E-Motor's rotor. Since it is not known, Variant three requires modification of YASA rotor to be hollow. In order to keep the axes from the differential towards from one of the wheels.

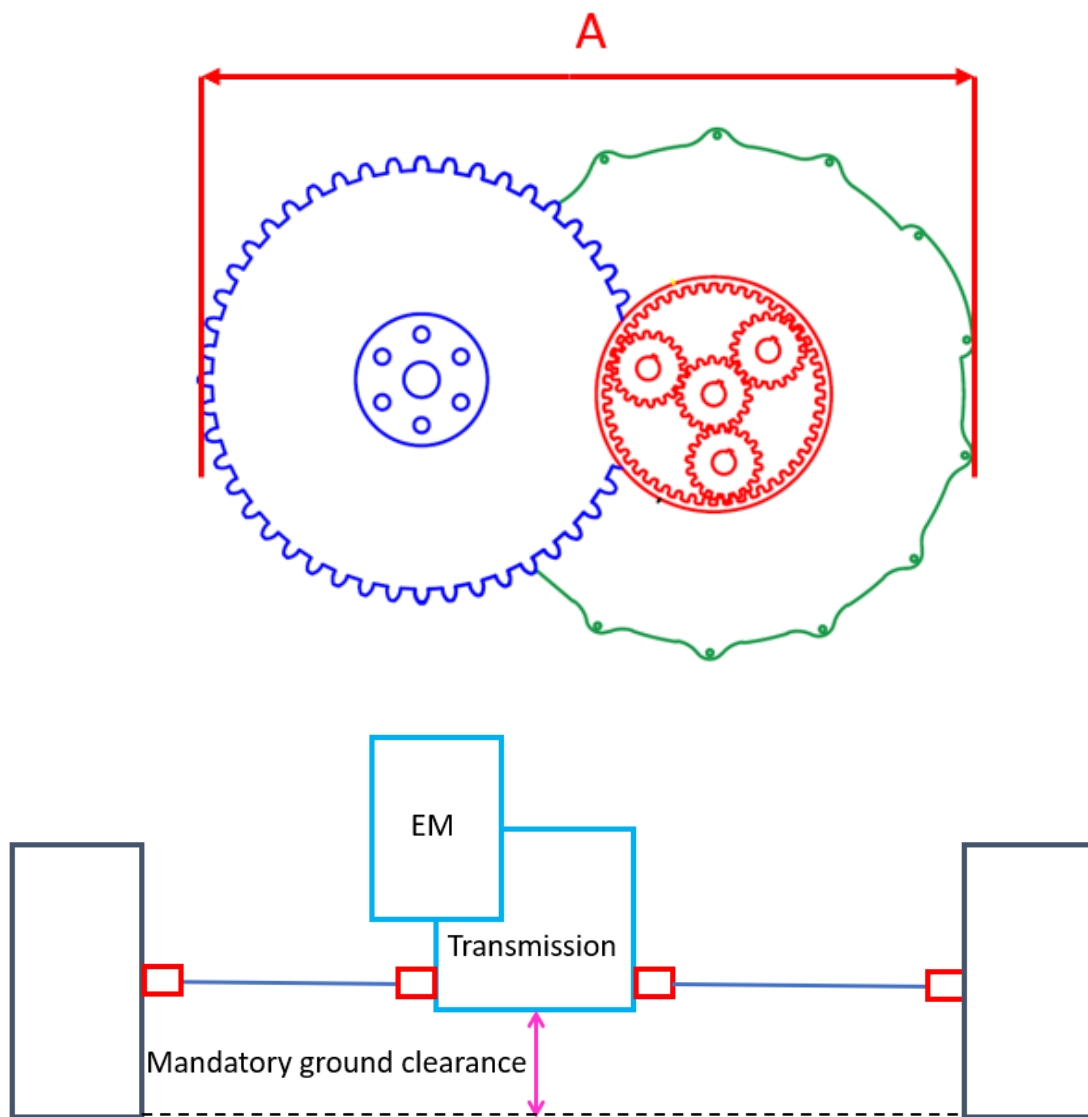


Fig. 41 Configuration of the Selected Variant

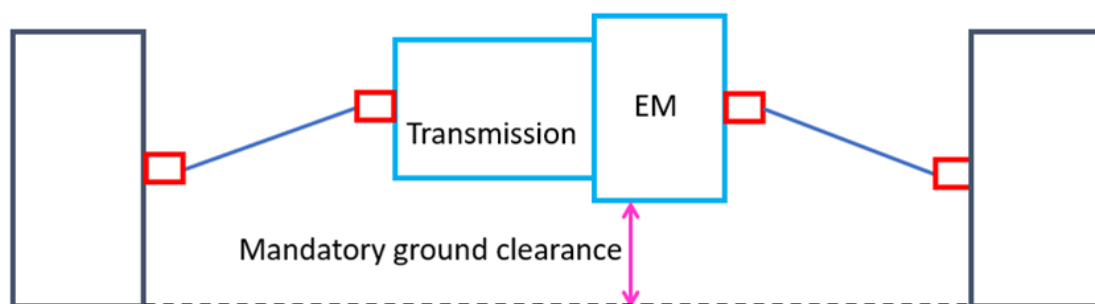


Fig. 40 Configuration of Variant Three



5.2. The Ratio and The Planet Diameters Calculation

In chapter three, with the given vehicle parameters the total ratio calculation have been done and it founded as $i=5.6737$. This ratio is total transmission ratio including the ratio of planetary gear set and the final drive ratio. The total transmission ratio is equal to the multiplication of the planetary gearset ratio and the final drive ratio.

$$i_{TOTAL} = i_{sun.carrier}^{ring} * i_{FD} \quad \text{Eq.24}$$

To be able to find the number of teeth of the planetary gearset components, the planetary gearset ratio must be found. The only known value is the total ratio, and as an engineering approach the final drive ratio could be estimated. The final drive ratio, can be chosen in a single step as $2 \leq i_{FD} \leq 7$ [30]. Ricardo suggests that the optimal final drive ratio varies between 2.1 to 2.5. As a result, the final drive ratio have been selected as $i_{FD}=2.2$ for the calculations.

From that ;

$$5.6737 = i_{sun.carrier}^{ring} * (2.2)$$
$$i_{sun.carrier}^{ring} = 2.578$$

The planetary gearset ratio have been found as $i_{sun.carrier}^{ring} = 2.578$.

The design engineers are using a distinct notation to determine the power flow through the planetary gear set. In the notification, subscripts and superscript are used in order to show input, output and fixed element in the PGS.

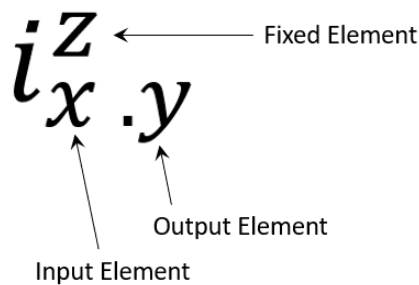


Fig. 42 Designation of Subscripts and Superscript



This ratio is the planetary gearset ratio when the sun is input, the carrier is output and the annulus (ring is stationary). So it could be written as ;

$$i_{PGS} = i_{sun.carrier}^{ring} = 2.578$$

5.2.1. The Basic Ratio of the Planetary Gearing

To be able to make a determination for the ratios, the geometrical parameters of the planetary gear systems are used. The determination is possible only for the mechanisms which have a fixed axis. In the analysis of the planetary gear drive trains, the carrier's rotation is restricted, by that way the drive train acts like a regular mechanism with fixed axis. By that way the pitch diameters or the number of teeth can be calculated. So the basic ratio is notated as ; $i_{sun.ring}^r$.

Now, to be able to continue the calculations; the basic ratio should be calculated. The basic ratio can be calculated by the help of the Willis formulas (sun is input, carrier is output and ring movement is restricted ($\omega_{ring}=0$));

$$i_{sun.ring}^{carrier} = \frac{\omega_{sun} - \omega_r}{\omega_{ring} - \omega_r} = -\frac{\omega_{sun} - \omega_r}{\omega_r} = 1 - \frac{\omega_{sun}}{\omega_r} \quad \text{Eq.25}$$

$$i_{sun.ring}^{carrier} = 1 - i_{sun.carrier}^{ring}$$

From that equation the basic ratio would be ;

$$i_{sun.ring}^{carrier} = 1 - 2.578$$

$$i_{sun.ring}^{carrier} = -1.578$$

The basic ratio is $i_{sun.ring}^{carrier} = 1.578$. The minus sign in the beginning means that the output rotates with a different sense of rotation than the input. It is called as negative ratio [31].

After the calculation of the basic ratio, the pitch diameter of the planetary gear system, and the numbers of teeth of each system can be calculated.



5.2.2. Pitch Diameter and Teeth Number Calculation of the Planetary Gearset Components

Since the basic ratio is known, now the pitch diameter of the components and the number of teeth of the components can be calculated.

To prevent any failure during operation, from comparison to other benchmarks; the diameter under bearing in the planet gear (pin diameter) must be higher than 10 millimeters. According to that information, the sun gear's pitch diameter is assumed as 110 millimeters (Fig 40. length A).

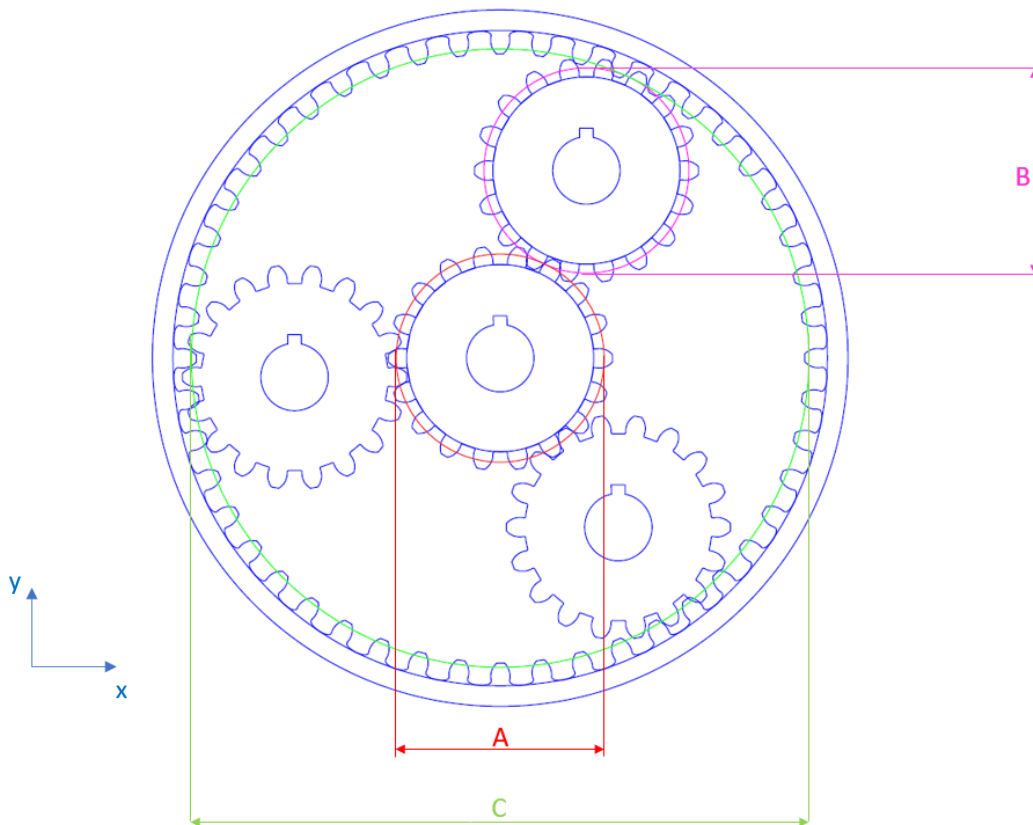


Fig. 43 Illustration for Showing the Pitch Diameters of the Components

The multiplication of basic ratio and the sun gear pitch diameter gives the pitch diameter of the ring gear. The result must be in the absolute value because ,the negative ratio only represents the direction of the output, which is the opposite direction of the input.



$$P_{ring} = |i_{sun.ring}^{carrier}| * P_{sun} \quad \text{Eq.26}$$

From this calculation the pitch circle diameter of the ring(Fig.40 length C) will be found as;

$$P_{ring} = 173.685 \text{ mm}$$

The difference between the ring pitch diameter and sun pitch diameter gives the pitch diameter of the planet gear(Fig. 40 length B) ;

$$P_{planet} = \frac{P_{ring} - P_{sun}}{2} \quad \text{Eq. 27}$$

From this calculation the pitch circle diameter of the planet will be found as;

$$P_{planet} = 31.8425 \text{ mm}$$

The module m is the ratio of the pitch diameter to the number of teeth. How big or small the gear is indicated by the module value. In this application the module m is accepted as 1.5 millimeters ($m=1.5 \text{ mm}$).

The gears which are used in the design is helical gears. The main reason why the helical gears are used is the effect of noise. Since the electric vehicles does not have an internal combustion engine, which is a source of noise, it is wanted that the transmissions for an electric vehicle operates as silent as possible.

Since the gears are helical, there must be the helix angle identification. The helix angle is the angle between the helix and an axial line on its right [33]. The standard helix angle application is between 15° to 30° for helical gears[34]. For our application the selected number of the helix angle is $\beta = 20^\circ$.



The tooth height (h) and the dedendum (h_f) are functions of module. They are calculated by ;

$$h = 2.5 * m \quad \text{Eq. 28}$$

$$h_f = 1.5 * m \quad \text{Eq. 29}$$

The dedendum and the tooth height are found as $h=3.75\text{mm}$ and $h_f=2.25\text{mm}$, respectively.

The root diameter of the planet can be found by the difference between the planet diameter and the dedendum diameter;

$$d_{ROOT} = P_{Planet} - 2 * h_f \quad \text{Eq. 30}$$

The needle bearing diameter which is going to be used inside of the planetary gearset is calculated by ;

$$d_{BEARING} = d_{ROOT} - 2 * 1.2 * h \quad \text{Eq. 31}$$

It is assumed that the roller in the needle bearing has size of 3 millimeters. And the diameter under the bearing is calculated by ;

$$d_{UB} = d_{BEARING} - 2 * d_{roller} \quad \text{Eq. 32}$$

As a result the root diameter found as $d_{ROOT} = 27.34 \text{ mm}$, the bearing diameter found as $d_{BEARING} = 18.34 \text{ mm}$,and the diameter under the bearing is found as; $d_{UB} = 12.34 \text{ mm}$ respectively. This calculation provides our necessary amount the diameter under the bearing must be higher than 10 millimeters. The bearing selection can be done according to this values calculated, from a catalog.



Since there are the pitch diameter and module values, the number of teeth of the each element can be calculated. The number of teeth can be found from the division of pitch diameter by the module. This calculation is valid for spur gears. For the helical gears the effect of the helix angle should be considered, and it changes the formula slightly as ;

$$z = \frac{P}{m} * \cos(\beta) \quad \text{Eq. 33}$$

When the formula is applied to the sun, planet and the ring gears they will be found as;

$$z_{sun} = 68.91 \text{ teeth}$$

$$z_{planet} = 19.94 \text{ teeth}$$

$$z_{ring} = 108.81 \text{ teeth}$$

The founded numbers are not integer, the numbers must be integer and, the condition for assembly of the planets must be considered. This condition is given by ;

$$\frac{z_{ring} + z_{sun}}{\#p} = \text{Integer} \quad \text{Eq. 34}$$

This equation is must be correct for the number of planets are equally spaced inside the set. So, there can be small distribution placed for the number of teeth by rounding off the numbers to the close integer value. The effect of rounding off has a very small effect on ratio, that it is acceptable.

When the teeth numbers are rounded off to an integer value they will be founded as ;

$$z_{sun} = 69 \text{ teeth}$$

$$z_{planet} = 20 \text{ teeth}$$

$$z_{ring} = 108 \text{ teeth}$$



If the condition is checked for the assemble ability of the planetary gearset with equispaced planets, when the aimed number of planets are using the system is going to be three ;

$$\frac{z_{ring} + z_{sun}}{\#p} = \frac{108 + 69}{3} = 59$$

The solution of the condition is 59, and thus it is an integer number, so the condition is fulfilled, and it is known that the assembly of the planetary gearset is possible.

5.2.3. Pitch Diameter and Teeth Number Calculations of the Final Drive

The final drive diameter and teeth number calculations are done with the same method as in the planetary gearset calculation. The only issue must be considered is, the center distance of the differential must be longer than the electric motor radius for prevent a collision and make the assembly possible.

The module and the helix angle selected differently for the Final Drive and the pinion pair; $m_{FD}=4$ mm, $\beta_{FD}=28^\circ$. The reason behind this is to keep the contact ratio from 3 to 4 to operate the gearsets as silent as possible. To keep the contact ratio high the width of the gears selected high as well.

First of all, it is necessary to calculate the centre distance that, the pitch diameters of the final drive and the pinion calculation possible.

Tab. 8 Required Parameters for Centre Distance Calculation

Electric Motor Radius	147 mm
Output Shaft Radius	15 mm
Clearance	15 mm

The centre distance is calculated as the summation of all three parameters are described in the Table 8. As a result , the centre distance is found as 177 milimeters. With this information obtained, the pitch diameter calculation for both final drive and the pinion can be done.



The ratio, and the center distances are known; so it can be said that the multiplication of the final drive ratio and the pinion pitch diameter gives the final drive pitch diameter. It is calculated as ;

$$\frac{d_1 + d_2}{2} = 177 \text{ mm}$$

$$d_1 * i_{FD} = d_2$$

From that calculation the pitch diameters of pinion and the final drive are calculated as;

$$d_1 = 110.625 \text{ mm}$$

$$d_2 = 243.375 \text{ mm}$$

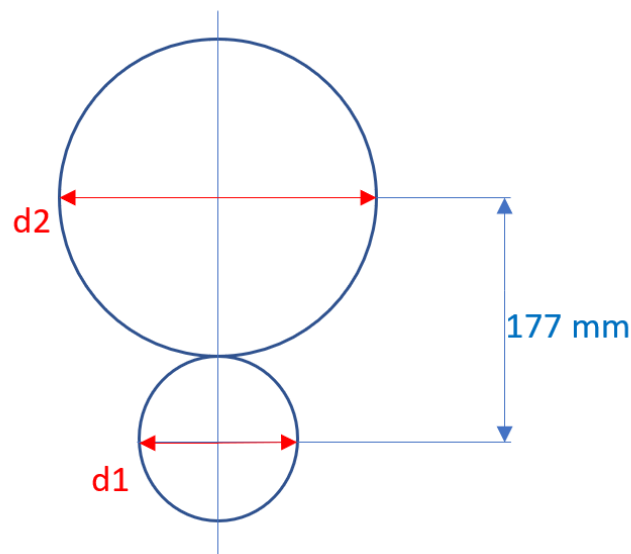


Fig. 44 Illustration of Final Drive and the Pinion Pitch Diameters

The number of teeth of pinion and the final drive is calculated from the equation 21, and from the equation the results are obtained as ;

$$z_{pinion} = 53.72 \approx 54 \text{ teeth}$$

$$z_{FD} = 24.419 \approx 25 \text{ teeth}$$



Tab. 9 Results of the Planetary Gearset Design Calculations

Planetary Gearset	Acronyms	-
Total Ratio	i_{TOTAL}	5.673
PGS Ratio	i_{PGS} OR $i_{sun}^{ring} \cdot carrier$	2.578
Basic Ratio	$i_{sun}^{carrier} \cdot ring$	-1.579
Module	m	1.5 mm
Sun Diameter	P_{SUN}	110 mm
Ring Diameter	P_{RING}	173.685 mm
Planet Diameter	P_{PLANET}	31.8425 mm
Tooth Height	h	3.75 mm
Dedendum	h_F	2.25 mm
Root diameter	d_{ROOT}	27.342 mm
Bearing Diameter	$d_{BEARING}$	18.3425 mm
Roller Size	d_{ROLLER}	3 mm
Dia.Under Bearing	d_{UB}	12.342 mm
Helix Angle	β	20 °
# of teeth of Sun	Z_{SUN}	69 teeth
# of teeth of Planet	Z_{PLANET}	20 teeth
# of teeth of Ring	Z_{RING}	108 teeth
Final Drive	-	-
Final Drive Ratio	i_{FD}	2.2
Electric Motor Radius	r_{MOTOR}	147 mm
Output shaft diameter	d_{OUTPUT}	30 mm
Clearance	clearance	15 mm
Center Distance	CD	177 mm
Final Drive Pitch Diameter	D_2	243.375 mm
Pinion Pitch Diameter	D_1	110.625 mm
# of teeth of Final Drive	Z_{FD}	54 teeth
# of teeth of Pinion	Z_{PINION}	25 teeth
Module	m_{FD}	4 mm
Helix angle	β_F	28 °



5.3. Strength Calculations of The Gear Meshes with SABR Software

After the geometrical properties are determined, the strength calculations of the planetary gearset prepared with the help of Ricardo Company's structural analysis software SABR/GEAR.

The software SABR/GEAR, checks the design's suitability to production, analyse and optimise the systems in terms of durability, friction, vibrations according to the standard: "ISO-6336 : Calculation of Load Capacity of Spur and Helical Gears".

The software SABR/GEAR provides the user to enter the basic geometry parameters, stress calculation inputs (such as microgeometry, facewidth, the axial location of the mesh etc.), the amount of backlash and a duty cycle, and according to the material which is used, it calculates the amount of stress (bending and contact stress of the gears, the amount of damage) and possible lifetime when it is applied to the gears, shaft and the bearings.

This software is applied first for the gear geometry, to the meshes between Sun/Planet, Planet/Ring and the Final Drive/Pinion.

5.3.1. Duty Cycle

The duty cycle of a transmission is defined as the speed and load conditions over which the transmission operates in a specific application. Understanding the speed and load history and preparing the design according to the application have crucial importance for transmission designers. The designers' expectation is for the transmission is completing their duty cycle in 250.000 kilometers accordingly. Ricardo uses „Speed-Up Duty Cycle“ which is also called Factored Duty Cycle. The engineers in Ricardo Prague are provided with the measured Duty Cycles in the conditions of Torques + Shafts speeds + Durations (Times). In other words, for each component in the transmission, which has a crucial importance is tested in maximum nominal and peak torques for a specific time. For the Planetary Gearset for Electric Vehicle application, the suggested duty cycle strategy is by Ricardo is described in Table 10.

Tab. 10 Ricardo's Suggested Duty Cycle Strategy for the Current Gearbox

BENDING STRESS	21h	Maximum Nominal Torque
	0.05h	Maximum Peak Torque
CONTACT STRESS	41h	Maximum Nominal Torque
	0.1h	Maximum Peak Torque
BEARING STRESS	244h	Maximum Nominal Torque
	0.0001h	Maximum Peak Torque



The screenshot displays the SABR software interface with various tabs and panels. The 'Duty Cycle' tab is active, showing input parameters and analysis results for Pinion and FD gears.

Optimisation Constraints:

Normal Landwidth	2.773 mm	3.098 mm
Minimum Landwidth	1.200 mm	1.200 mm
Fillet Clearance	0.541 mm	1.094 mm
Minimum Fillet Clearance	0.150 mm	
Root Clearance	1.966 mm	1.966 mm
Minimum Root Clearance	0.662 mm	

Quality Ratios:

Transv. Contact Ratio, ϵ_α	1.455	
Helical Overlap Ratio, ϵ_β	2.017	
Total Contact Ratio, ϵ_γ	3.472	
Rel. Slide Velocity Ratio	1.201	
SAP Specific Slide Ratio	1.158	1.029

Duty Cycle Parameters:

- Pinion Input Torque - Speed: 953.000 Nm, 3102.000 rpm
- Pinion Input Torque Direction: POSITIVE
- Duration / Required Life: 0.100 hour
- Reverse Bending: Driver (selected), NOT Driver
- ISO Tangential Velocity: 18.195 m/s
- Tangential Tooth Force: 1.701E4 N
- Axial Tooth Force: 8948.128 N
- Separating Tooth Force: 6470.222 N

Analysis Results Table:

	Pinion	FD
ISO Nom. Bending Stress σ_{FO}	154.079 MPa	159.016 MPa
ISO Actual Bending Stress σ_F	251.081 MPa	259.127 MPa
ISO Permissible Stress σ_{FP}	1551.732 MPa	1644.681 MPa
ISO Bending Life	INFINITE hour	INFINITE hour
ISO Bending Damage	0.000 %	0.000 %
ISO Safety Factor SF	6.180	6.347
ISO Actual Contact Stress σ_{H1}	1007.985 MPa	1007.985 MPa
ISO Permissible Stress σ_{HP}	2400.000 MPa	2400.000 MPa
ISO Contact Life	INFINITE hour	INFINITE hour
ISO Contact Damage	0.000 %	0.000 %
ISO Safety Factor SH	2.381	2.381

Fig. 45 Screenshot of Ricardo Software SABR

5.3.2. Material Properties of the Components

The aimed material for production is the case hardened steel 27MnCr5.

This alloyed heat treatable steel is used for parts requiring high surface wear resistance but having a soft core which absorb stresses without cracking. 27MnCr5 is widely used in automotive industry for many applications, such as in the production of axles, shafts, pinions and gears.

To be able to know the strength of the material during application, it is required to know the material properties. The properties are described in Table 11.



Tab. 11 Material Properties of 27MnCr5

Material Name	27MnCr5
Young's Modulus	206 GPa
Density	7800 kg/m ³
Bending Yield Stress	1150 MPa
Contact Yield Stress	2400 MPa
Bending Stress Limit	558 MPa
Contact Stress Limit	1190 MPa
Surface Hardness HRC	61 RC
Brinell / Vickers Hardness	670/720

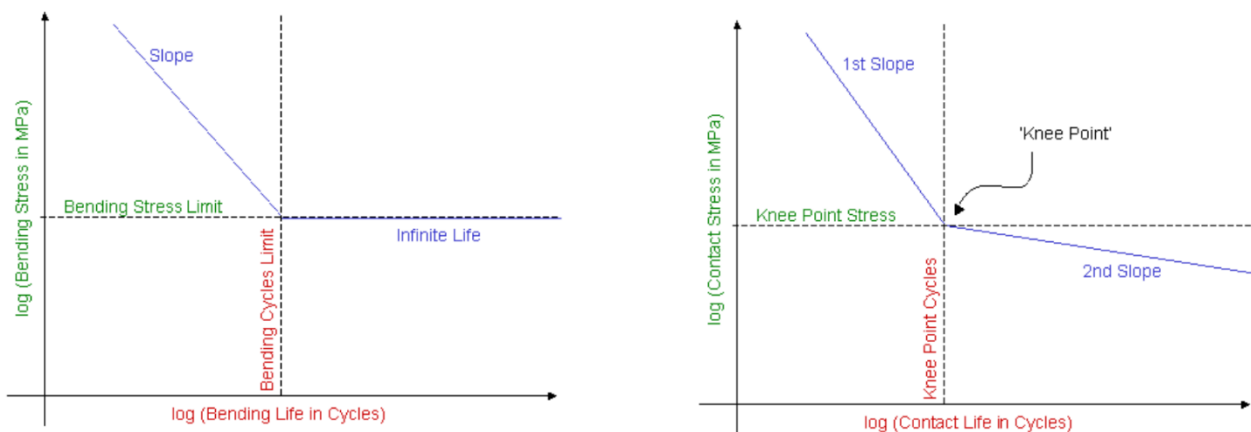


Fig. 46 S-N Curve of 27MnCr5 for Bending Stress and Contact Stress [34]

The aim is being in the zone which is lower than the stress limit to reach the infinite life. Since the material properties which is going to be used is known, the results of bending and the contact stresses which are affecting the gears are understandable. Each component mesh in the gearbox design is simulated with the recommended duty cycle strategy for this specific case by Ricardo; Bending Stress and Contact Stresses determined in the Maximum Nominal Torque and Maximum Peak Torque.



5.3.3. Sun/Planet Mesh Results

First application is done for the Sun/Planet arrangement.

The basic geometry parameters entered the software and the microgeometry features (such as max/min chamfer tip.) accepted as constant in all variants.

Parameter	Value	Unit
Mesh Type	<input checked="" type="radio"/> Sun/Planet	
Gear Names	Sun / Planet	
Sun/Planet	is Sun / is Planet	
Number of Planets	3	
Planet Load Share	<input checked="" type="radio"/> Unequal Load Share	
Number of Teeth, z	69 / 20	
ISO Pinion	FALSE / TRUE	
Default Gear Ratio	0.290	
Normal Module, mn	1.500	mm
Normal Pressure Angle, α_n	20.000	°
Helix Angle, β	20.000	°
Helix Hand	LEFT / RIGHT	
Centre Distance, a	70.910	mm
Total Profile Shift Coefficient	-0.082	

Fig. 47 Basic Geometry Features in Sun/Planet Configuration in SABR/GEAR

Parameter	Value	Unit
Default Reverse Bending	<input checked="" type="radio"/> NO	
Default Driver	Driver / NOT Driver	
Max. Tip Chamfer	0.100	mm
Min. Tip Chamfer	0.050	mm
Facewidth	34.000	mm
Axial Location	0.000	mm
Facewidth Overlap	32.000	mm
Overlapping Facewidth, b	32.000	mm
Active Facewidth	34.000 / 32.000	mm
Tolerance on OD	0.100	mm
Profile Shift (Zero Backlash)	0.000 / -0.123	mm
Profile Shift Coefficient	0.000 / -0.082	
Dedendum, hf	1.500	mm
Outside Diameter (ha=1)	113.142 / 34.679	mm
Outside Diameter, da	113.142 / 34.679	mm
Addendum, ha	1.000	mm
Max. Tool Radius (per module)	0.342	mm
Actual Tool Radius (per module)	0.342	mm
Enter Circumferential / Normal	<input checked="" type="radio"/> Circumferential	
Gear max circumferential Backlash	0.075	mm
Gear min circumferential Backlash	0.025	mm
Pair max circumferential backlash	0.150	mm
Pair min circumferential backlash	0.050	mm
Profile Shift for Max. Backlash	-0.097	mm
Profile Shift for Min. Backlash	-0.032	mm
Min. Centre Distance	70.910	mm
Min. Extreme Backlash	50.000	µm

Fig. 48 The Inputs for Microgeometry and Backlash in SABR/GEAR



With the specific data entered for the Maximum Nominal and Maximum Peak Torque, the results are obtained for the four cases;

Tab. 12 Entered Duty Cycle Properties For Sun/Planet Mesh

Peak Torque on Sun Gear		370 Nm
Nominal Torque on Sun Gear		200 Nm
Sun Shaft Speed		8000 rpm
Carrier Speed		3103 rpm
BENDING	Nominal Torque Duration	21 hours
	Maximum Torque Duration	0.05 hours
CONTACT	Nominal Torque Duration	41 hours
	Maximum Torque Duration	0.1 hours

RICARDO ISO 6336		Sun		Planet	
ISO Nom. Bending Stress σ_{FO}	69.971	MPa	85.290	MPa	
ISO Actual Bending Stress σ_F	267.612	MPa	326.202	MPa	
ISO Permissible Stress σ_{FP}	849.107	MPa	587.291	MPa	
ISO Bending Life	INFINITE	hour	INFINITE	hour	
ISO Bending Damage	0.000	%	0.000	%	
ISO Safety Factor SF	3.173		1.800		
ISO Actual Contact Stress σ_H	1033.732	MPa	1033.732	MPa	
ISO Permissible Stress σ_{HP}	1495.514	MPa	1476.698	MPa	
ISO Contact Life	INFINITE	hour	INFINITE	hour	
ISO Contact Damage	0.000	%	0.000	%	
ISO Safety Factor SH	1.447		1.429		
RICARDO ISO 6336		Sun		Planet	
ISO Nom. Bending Stress σ_{FO}	129.446	MPa	157.787	MPa	
ISO Actual Bending Stress σ_F	359.316	MPa	437.983	MPa	
ISO Permissible Stress σ_{FP}	1448.962	MPa	902.089	MPa	
ISO Bending Life	INFINITE	hour	INFINITE	hour	
ISO Bending Damage	0.000	%	0.000	%	
ISO Safety Factor SF	4.033		2.060		
ISO Actual Contact Stress σ_H	1197.825	MPa	1197.825	MPa	
ISO Permissible Stress σ_{HP}	2400.000	MPa	2400.000	MPa	
ISO Contact Life	4186.318	hour	3640.277	hour	
ISO Contact Damage	0.001	%	0.001	%	
ISO Safety Factor SH	2.004		2.004		
ISO 6336 Edition		ISO 6336:2006 Corr. 2...			

Fig. 49 Results for Bending in Nominal(Above) and Maximum Torque(Below)



RICARDO ISO 6336		Sun		Planet	
ISO Nom. Bending Stress σ_{FO}	69.971	MPa	85.290	MPa	
ISO Actual Bending Stress σ_F	267.612	MPa	326.202	MPa	
ISO Permissible Stress σ_{FP}	837.801	MPa	579.472	MPa	
ISO Bending Life	INFINITE	hour	INFINITE	hour	
ISO Bending Damage	0.000	%	0.000	%	
ISO Safety Factor SF	3.131		1.776		
ISO Actual Contact Stress σ_H	1033.732	MPa	1033.732	MPa	
ISO Permissible Stress σ_{HP}	1407.558	MPa	1389.848	MPa	
ISO Contact Life	INFINITE	hour	INFINITE	hour	
ISO Contact Damage	0.000	%	0.000	%	
ISO Safety Factor SH	1.362		1.344		
RICARDO ISO 6336		Sun		Planet	
ISO Nom. Bending Stress σ_{FO}	129.446	MPa	157.787	MPa	
ISO Actual Bending Stress σ_F	359.316	MPa	437.983	MPa	
ISO Permissible Stress σ_{FP}	1335.180	MPa	844.277	MPa	
ISO Bending Life	INFINITE	hour	INFINITE	hour	
ISO Bending Damage	0.000	%	0.000	%	
ISO Safety Factor SF	3.716		1.928		
ISO Actual Contact Stress σ_H	1197.825	MPa	1197.825	MPa	
ISO Permissible Stress σ_{HP}	2400.000	MPa	2397.048	MPa	
ISO Contact Life	4186.318	hour	3640.277	hour	
ISO Contact Damage	0.002	%	0.003	%	
ISO Safety Factor SH	2.004		2.001		
ISO 6336 Edition		ISO 6336:2006 Corr. 2...			

Fig. 50 Results for Contact in Nominal(Above) and Maximum Torque(Below)

- When the results obtained for the Bending Stress, the results are applicable and lower for the material's stress bending limit.
- The software shows that both Sun and Planet gears can be used theoretically in infinite lifetime, without a bending damage.
- When the results obtained for the Contact Stress, the results are applicable and low for the material's fatigue limit.
- The software shows that both Sun and Planet gears can be used theoretically in infinite lifetime in nominal torque, but when the maximum peak torque applied, the contact life becomes determinable and micro damages occur in both Sun and Planet Gears.



5.3.4. Planet/Annulus(Ring) Mesh Results

Second application is done for Planet/Ring Mesh arrangement.

Tab. 13 Entered Duty Cycle Properties For Planet/Ring Mesh

Peak Torque on Ring		1276.5 Nm
Nominal Torque on Ring		690 Nm
Carrier Speed		3103 rpm
Ring(Annulus)Speed		0 rpm (stationary)
BENDING	Nominal Torque Duration	21 hours
	Maximum Torque Duration	0.05 hours
CONTACT	Nominal Torque Duration	41 hours
	Maximum Torque Duration	0.1 hours

With the specific data entered for the Maximum Nominal and Maximum Peak Torque, the results are obtained for the four cases;

	Planet		Annulus	
ISO Nom. Bending Stress σ_{FO}	173.634	MPa	149.712	MPa
ISO Actual Bending Stress σ_F	467.648	MPa	403.219	MPa
ISO Permissible Stress σ_{FP}	589.760	MPa	870.262	MPa
ISO Bending Life	INFINITE	hour	INFINITE	hour
ISO Bending Damage	0.000	%	0.000	%
ISO Safety Factor SF	1.261		2.158	
ISO Actual Contact Stress σ_H	991.175	MPa	991.175	MPa
ISO Permissible Stress σ_{HP}	1496.417	MPa	1576.095	MPa
ISO Contact Life	INFINITE	hour	INFINITE	hour
ISO Contact Damage	0.000	%	0.000	%
ISO Safety Factor SH	1.510		1.590	
ISO 6336 Edition	ISO 6336:2006 Corr. 2...			

Fig. 51 Results for Bending Stress in Nominal Torque



RICARDO		ISO 6336		
	Planet		Annulus	
ISO Nom. Bending Stress σ_{FO}	321.222	MPa	276.966	MPa
ISO Actual Bending Stress σ_F	637.301	MPa	549.498	MPa
ISO Permissible Stress σ_{FP}	948.500	MPa	1762.058	MPa
ISO Bending Life	2.081	hour	INFINITE	hour
ISO Bending Damage	2.403	%	0.000	%
ISO Safety Factor SF	1.488		3.207	
ISO Actual Contact Stress σ_H	1157.078	MPa	1157.078	MPa
ISO Permissible Stress σ_{HP}	2400.000	MPa	2400.000	MPa
ISO Contact Life	INFINITE	hour	INFINITE	hour
ISO Contact Damage	0.000	%	0.000	%
ISO Safety Factor SH	2.074		2.074	
ISO 6336 Edition		ISO 6336:2006 Corr. 2...		

Fig. 52 Results for Bending Stress in Maximum Torque

RICARDO		ISO 6336		
	Planet		Annulus	
ISO Nom. Bending Stress σ_{FO}	178.619	MPa	148.176	MPa
ISO Actual Bending Stress σ_F	477.365	MPa	396.003	MPa
ISO Permissible Stress σ_{FP}	580.328	MPa	858.580	MPa
ISO Bending Life	INFINITE	hour	INFINITE	hour
ISO Bending Damage	0.000	%	0.000	%
ISO Safety Factor SF	1.216		2.168	
ISO Actual Contact Stress σ_H	970.291	MPa	970.291	MPa
ISO Permissible Stress σ_{HP}	1410.614	MPa	1485.723	MPa
ISO Contact Life	INFINITE	hour	INFINITE	hour
ISO Contact Damage	0.000	%	0.000	%
ISO Safety Factor SH	1.454		1.531	

RICARDO		ISO 6336		
	Planet		Annulus	
ISO Nom. Bending Stress σ_{FO}	330.446	MPa	274.125	MPa
ISO Actual Bending Stress σ_F	651.693	MPa	540.618	MPa
ISO Permissible Stress σ_{FP}	858.932	MPa	1601.882	MPa
ISO Bending Life	1.582	hour	INFINITE	hour
ISO Bending Damage	6.323	%	0.000	%
ISO Safety Factor SF	1.318		2.963	
ISO Actual Contact Stress σ_H	1133.700	MPa	1133.700	MPa
ISO Permissible Stress σ_{HP}	2398.865	MPa	2400.000	MPa
ISO Contact Life	INFINITE	hour	INFINITE	hour
ISO Contact Damage	0.000	%	0.000	%
ISO Safety Factor SH	2.116		2.117	
ISO 6336 Edition		ISO 6336:2006 Corr. 2...		

Fig. 53 Results for Contact in Nominal(Above) and Maximum Torque(Below)



•When the results obtained for the Bending Stress, the results are applicable and lower for the material's stress bending limit in Nominal Torque. When the peak torque is applied, the bending stress limit is achieved for annulus gear, and ring is damaged 2.4 percentage.

• The software shows that both Ring and Planet gears can be used theoretically in infinite lifetime, without a bending damage in nominal torque, but in peak torque, ring has a finite life.

•The software shows that both Ring and Planet gears can be used theoretically in infinite lifetime in nominal torque, the contact stress limit is higher than the results.

5.3.5. Final Drive/Pinion Mesh Results

Third application is done for the Final Drive/Pinion mesh.

Tab. 14 Entered Duty Cycle Properties for Final Drive / Pinion Mesh

Peak Torque on Pinion		953 Nm
Nominal Torque on Pinion		515.6 Nm
Pinion Speed		3103 rpm
BENDING	Nominal Torque Duration	21 hours
	Maximum Torque Duration	0.05 hours
CONTACT	Nominal Torque Duration	41 hours
	Maximum Torque Duration	0.1 hours

With the specific data entered for the Maximum Nominal and Maximum Peak Torque, the results are obtained for the four cases;



RICARDO		ISO 6336		
	Pinion		FD	
ISO Nom. Bending Stress σ_{FO}	83.361	MPa	86.032	MPa
ISO Actual Bending Stress σ_F	169.886	MPa	175.330	MPa
ISO Permissible Stress σ_{FP}	871.838	MPa	924.496	MPa
ISO Bending Life	INFINITE	hour	INFINITE	hour
ISO Bending Damage	0.000	%	0.000	%
ISO Safety Factor SF	5.132		5.273	
ISO Actual Contact Stress σ_H	829.136	MPa	829.136	MPa
ISO Permissible Stress σ_{HP}	1739.389	MPa	1861.099	MPa
ISO Contact Life	INFINITE	hour	INFINITE	hour
ISO Contact Damage	0.000	%	0.000	%
ISO Safety Factor SH	2.098		2.245	
ISO 6336 Edition		ISO 6336:2006 Corr. 2...		

RICARDO		ISO 6336		
	Pinion		FD	
ISO Nom. Bending Stress σ_{FO}	154.079	MPa	159.016	MPa
ISO Actual Bending Stress σ_F	251.081	MPa	259.127	MPa
ISO Permissible Stress σ_{FP}	1677.448	MPa	1772.198	MPa
ISO Bending Life	INFINITE	hour	INFINITE	hour
ISO Bending Damage	0.000	%	0.000	%
ISO Safety Factor SF	6.681		6.839	
ISO Actual Contact Stress σ_H	1007.985	MPa	1007.985	MPa
ISO Permissible Stress σ_{HP}	2400.000	MPa	2400.000	MPa
ISO Contact Life	INFINITE	hour	INFINITE	hour
ISO Contact Damage	0.000	%	0.000	%
ISO Safety Factor SH	2.381		2.381	
ISO 6336 Edition		ISO 6336:2006 Corr. 2...		

Fig. 54 Results for Bending in Nominal(Above) and Maximum Torque(Below)



RICARDO		ISO 6336		
	Pinion		FD	
ISO Nom. Bending Stress σ_{FO}	83.361	MPa	86.032	MPa
ISO Actual Bending Stress σ_F	169.886	MPa	175.330	MPa
ISO Permissible Stress σ_{FP}	860.229	MPa	872.627	MPa
ISO Bending Life	INFINITE	hour	INFINITE	hour
ISO Bending Damage	0.000	%	0.000	%
ISO Safety Factor SF	5.064		4.977	
ISO Actual Contact Stress σ_H	829.136	MPa	829.136	MPa
ISO Permissible Stress σ_{HP}	1640.132	MPa	1754.896	MPa
ISO Contact Life	INFINITE	hour	INFINITE	hour
ISO Contact Damage	0.000	%	0.000	%
ISO Safety Factor SH	1.978		2.117	
ISO 6336 Edition	ISO 6336:2006 Corr. 2... ▼			

Fig. 55 Results for Contact Stress in Nominal Torque

RICARDO		ISO 6336		
	Pinion		FD	
ISO Nom. Bending Stress σ_{FO}	154.079	MPa	159.016	MPa
ISO Actual Bending Stress σ_F	251.081	MPa	259.127	MPa
ISO Permissible Stress σ_{FP}	1551.732	MPa	1644.681	MPa
ISO Bending Life	INFINITE	hour	INFINITE	hour
ISO Bending Damage	0.000	%	0.000	%
ISO Safety Factor SF	6.180		6.347	
ISO Actual Contact Stress σ_H	1007.985	MPa	1007.985	MPa
ISO Permissible Stress σ_{HP}	2400.000	MPa	2400.000	MPa
ISO Contact Life	INFINITE	hour	INFINITE	hour
ISO Contact Damage	0.000	%	0.000	%
ISO Safety Factor SH	2.381		2.381	
ISO 6336 Edition	ISO 6336:2006 Corr. 2... ▼			

Fig. 56 Results For Contact Stress in Maximum Torque

- When the results obtained for the Bending Stress, the results are applicable and lower for the material's stress bending limit in Nominal Torque and Peak Torque.
- The software shows that both Final Drive and Pinion gears can be used theoretically in infinite lifetime, without a bending damage in nominal torque and peak torque.
- The software shows that both Final Drive and Pinion gears can be used theoretically in infinite lifetime in nominal torque, the contact stress limit is higher than the results.



5.4. Strength Calculations of the Components with SABR Software

The strength calculations of the meshes for Bending and Contact Stresses are done with SABR software. In this section with SABR software, strength calculations of the assembly will be done.

In this chapter the strength results of the shafts and bearings will be discussed.

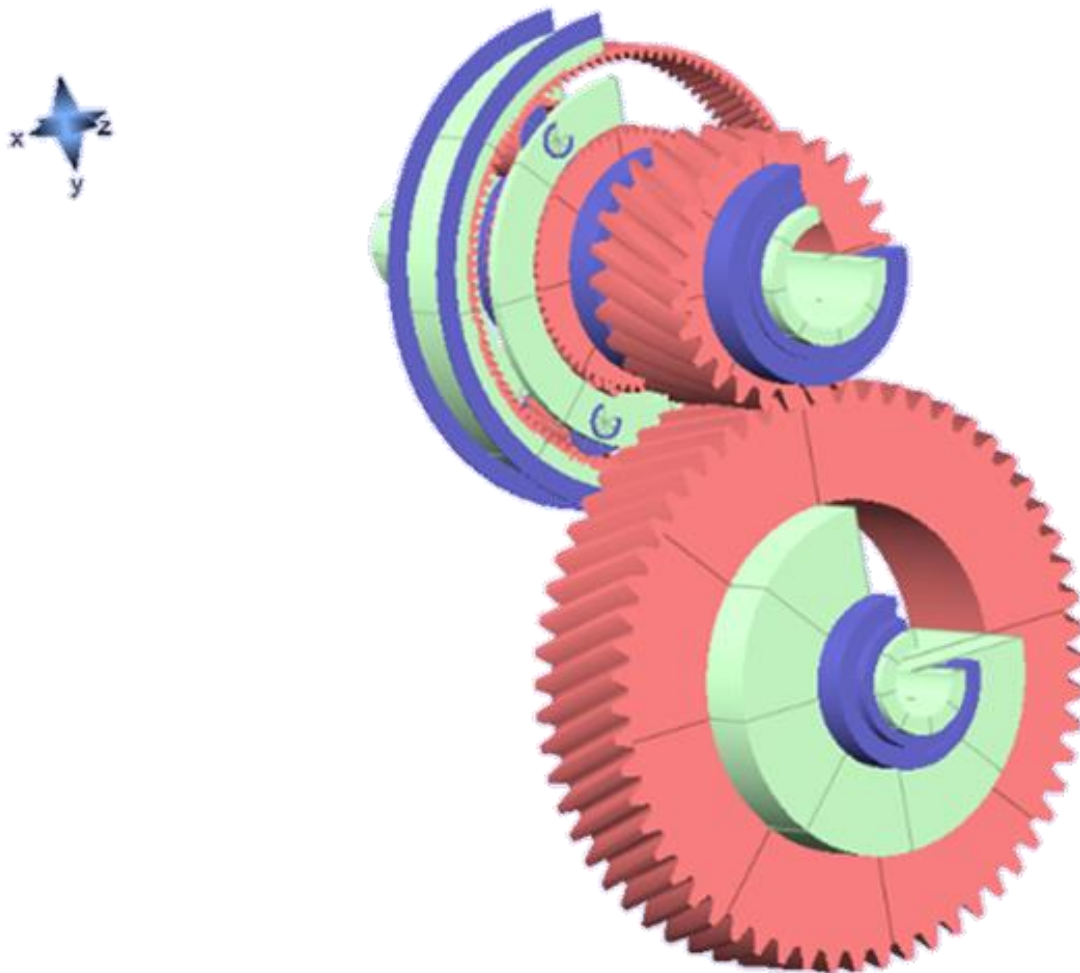


Fig. 57 Screenshot from the SABR Software



5.4.1. Bearing Selection

In the assembly used bearings are given in the Table 15.

Tab. 15 The Bearings Which are Used in The Assembly

Bearing Name In the SW	Bearing Catalog ID Name	Type of Bearing
BSun1	SKF-6209 [35]	Deep Groove Ball Bearing
BSun2	SKF-K455017 [36]	Needle Roller and Cage Bearing
Carrier Bearing1	SKF-6013Z [37]	Deep Groove Ball Bearing
Carrier Bearing2	SKF-6012 [38]	Deep Groove Ball Bearing
Bearing Differential1	SKF 32009 [39]	Tapered Roller Bearing
Bearing Differential2	SKF 32009 [39]	Tapered Roller Bearing
Planetary Gearset psa1	SKF K121812TN [40]	Needle Roller and Cage Bearing
Planetary Gearset Psa2	SKF K121812TN [40]	Needle Roller and Cage Bearing
Planetary Gearset psa3	SKF K121812TN [40]	Needle Roller and Cage Bearing

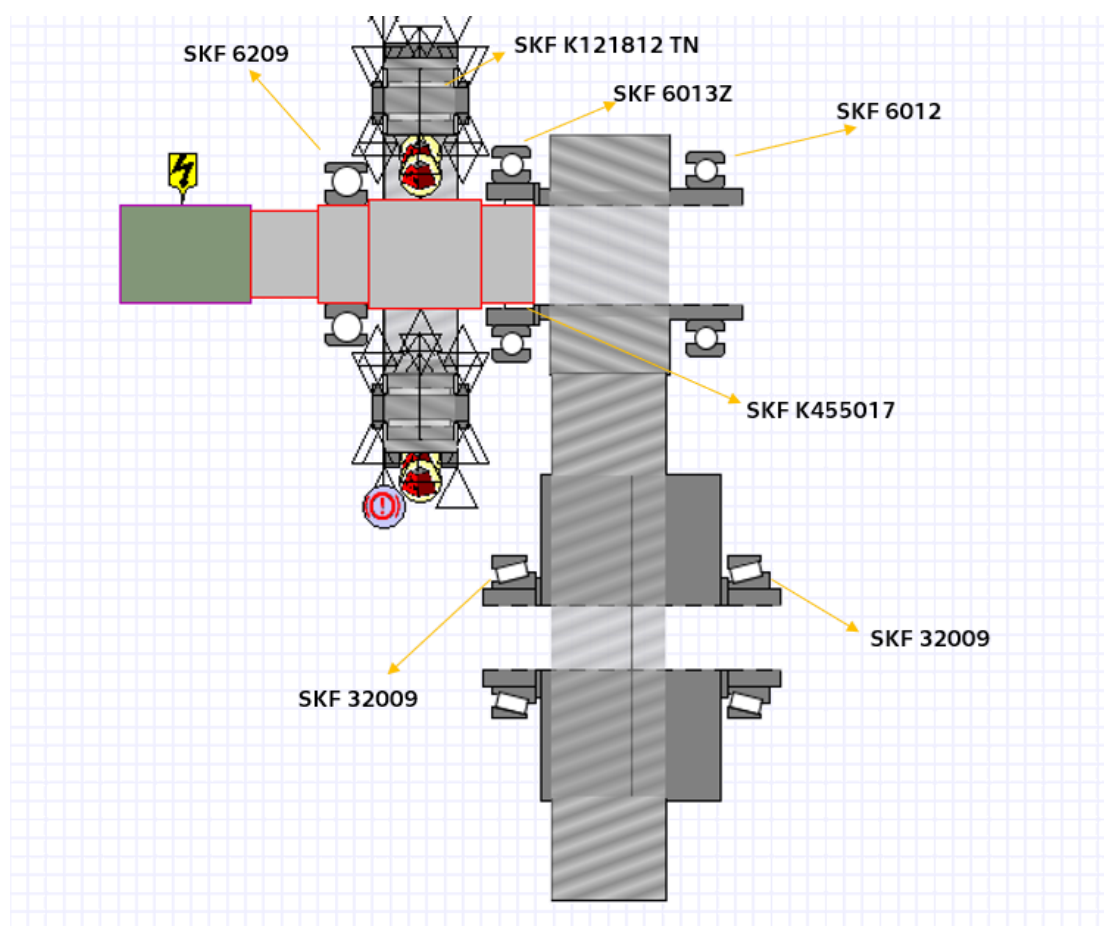


Fig. 58 Locations of The Bearings in the Assembly



5.4.2. Bearing Life and Temperature

Tab. 16 The Applied Stress/ Amount of Damage on Bearings

Bearing Name In the SW	Type	Life (hrs.)	Detailed Damage	Max. Stress (GPa)
BSun1	DG Ball	7083.6	3.4%	1.844
BSun2	CE Needle	INFINITE	0.0%	0.434
Carrier Bearing1	DG Ball	3223.4	7.6%	2.499
Carrier Bearing2	DG Ball	413.4	59%	3.221
Bearing Differential1	Tapered	7698.6	3.2%	2.628
Bearing Differential2	Tapered	68375.2	0.4%	2.041
Planetary Gearset psa1	CE Needle	673.3	36.2%	2.500
Planetary Gearset Psa2	CE Needle	648	37.7%	2.536
Planetary Gearset psa3	CE Needle	611.7	39.9%	2.539

As it can be seen from the Table 16, although the bearings are exposure to high stress levels, they will not have malfunction and can continue their operation.(see **Fig 57**) .

Bearing	Sealed	Lubricant	Flow Rate (L/min)	Max Temp. (°C)
BSun1	<input type="checkbox"/>	<input checked="" type="radio"/> Std Mineral Oil	<input checked="" type="radio"/> 0.200	106.730
BSun2	<input type="checkbox"/>	<input checked="" type="radio"/> Std Mineral Oil	<input type="radio"/> 0.100	90.325
Carrier Bearing 1	<input type="checkbox"/>	<input checked="" type="radio"/> Std Mineral Oil	<input checked="" type="radio"/> 0.200	109.462
Carrier Bearing 2	<input type="checkbox"/>	<input checked="" type="radio"/> Std Mineral Oil	<input checked="" type="radio"/> 0.350	108.519
Bearing Differential1	<input type="checkbox"/>	<input checked="" type="radio"/> Std Mineral Oil	<input checked="" type="radio"/> 0.200	106.137
Bearing Differential 2	<input type="checkbox"/>	<input checked="" type="radio"/> Std Mineral Oil	<input type="radio"/> 0.100	105.345
Planetary Gearset.psa1.planetBrg1	<input type="checkbox"/>	<input checked="" type="radio"/> Std Mineral Oil	<input checked="" type="radio"/> 0.200	108.121
Planetary Gearset.psa1.planet.thrustL	<input type="checkbox"/>	<input checked="" type="radio"/> Std Mineral Oil	<input type="radio"/> 0.100	90.000
Planetary Gearset.psa1.planet.thrustR	<input type="checkbox"/>	<input checked="" type="radio"/> Std Mineral Oil	<input type="radio"/> 0.100	90.000
Planetary Gearset.psa2.planetBrg1	<input type="checkbox"/>	<input checked="" type="radio"/> Std Mineral Oil	<input checked="" type="radio"/> 0.200	108.121
Planetary Gearset.psa2.planet.thrustL	<input type="checkbox"/>	<input checked="" type="radio"/> Std Mineral Oil	<input type="radio"/> 0.100	90.000
Planetary Gearset.psa2.planet.thrustR	<input type="checkbox"/>	<input checked="" type="radio"/> Std Mineral Oil	<input type="radio"/> 0.100	90.000
Planetary Gearset.psa3.planetBrg1	<input type="checkbox"/>	<input checked="" type="radio"/> Std Mineral Oil	<input checked="" type="radio"/> 0.200	108.122
Planetary Gearset.psa3.planet.thrustL	<input type="checkbox"/>	<input checked="" type="radio"/> Std Mineral Oil	<input type="radio"/> 0.100	90.000
Planetary Gearset.psa3.planet.thrustR	<input type="checkbox"/>	<input checked="" type="radio"/> Std Mineral Oil	<input type="radio"/> 0.100	90.000

Fig. 59 Maximum Bearing Temperature Simulation

Increase of temperature on bearings is an unwanted situation and by the SABR software, the maximum temperature of the bearings could reach simulated accordingly. The bearing temperatures above 110°C is not desired that, for the bearings which are achieving the amount, the flow rate of the of the coolant oil is increased.



5.4.3. Deflections on Shaft

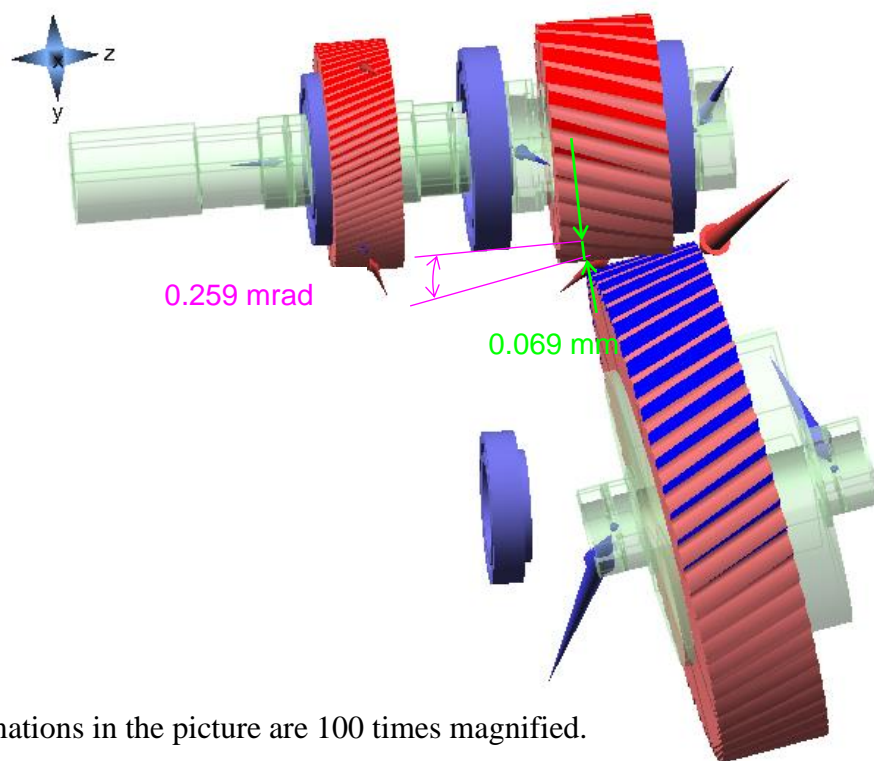
After the simulation is done ,the results are obtained for the deflection of the Shafts which can be seen in the Table 17.

Tab. 17 Maximum Radial Deflection By Load Case

Load Case/Shaft (μm)	Sun	Differential	Carrier	Pin1	Pin 2	Pin3
Nominal Torque	0.0	0.03	0.03	0.02	0.02	0.02
Peak Torque	0.0	0.05	0.05	0.03	0.03	0.03

By this part of the analysis, the areas which may have high stress can be detected. A deflection of 0.8 micron per mm deflection is acceptable by the Ricardo company that, all of the deflection values are within the limits.

For the nominal torque case we are concerned about the pinion and the wheel of the final drive. Therefore we checked the detailed figures for the center distance displacement as well as load of action misalignment (LOAMA) and the results are shown in the Table 18 and the pictures 57. As a result displacement is simulated as 0.069 microns and the slope is 0.259 mrad.



The deformations in the picture are 100 times magnified.

Fig. 60 LOMA and CD Displacement in FD and Pinion Mesh



The displacements of the differential and the carrier shaft are described on Figure 58 and Figure 59.

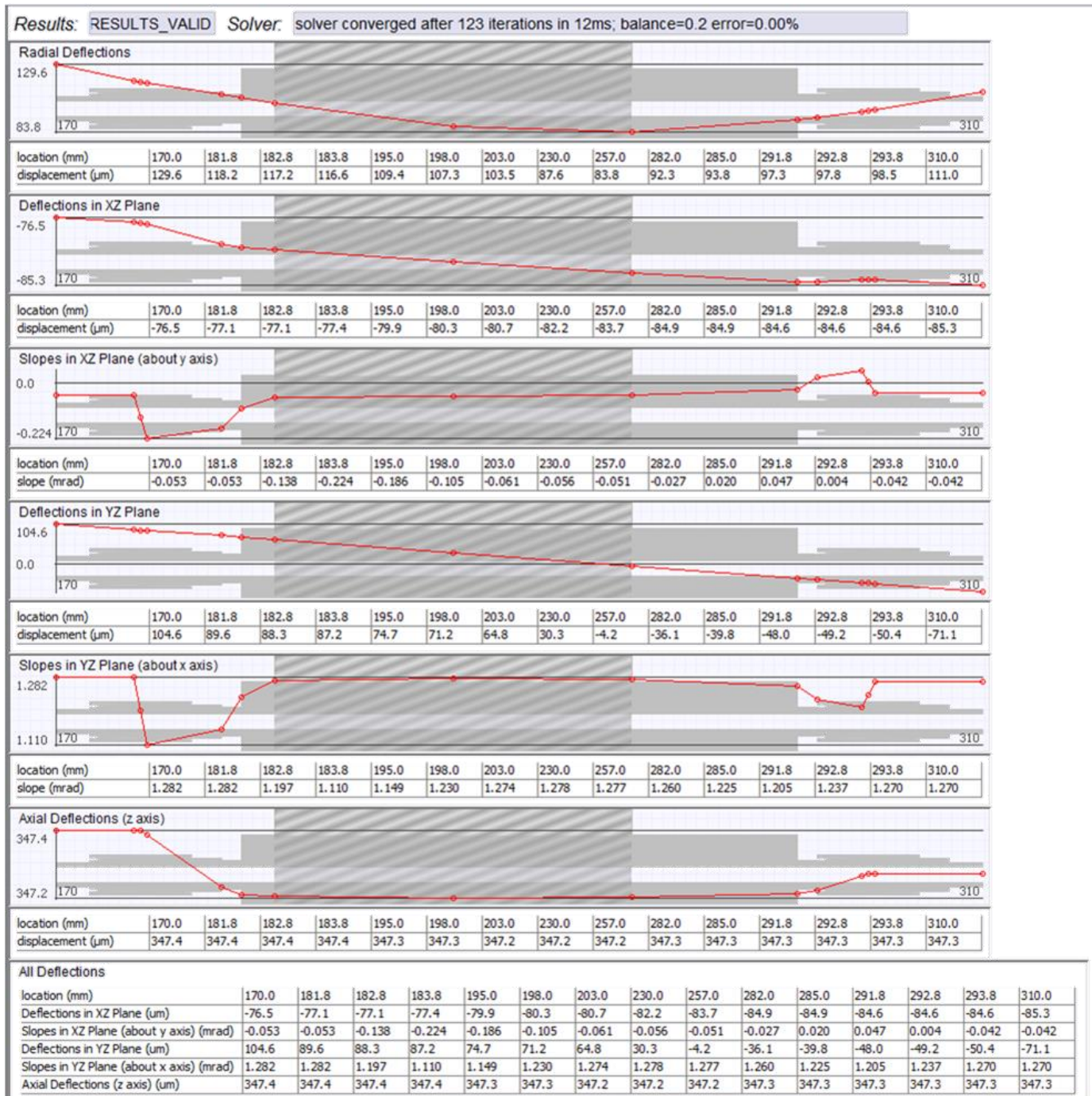


Fig. 61 Slopes and Deflections of the Differential with Respect to Location

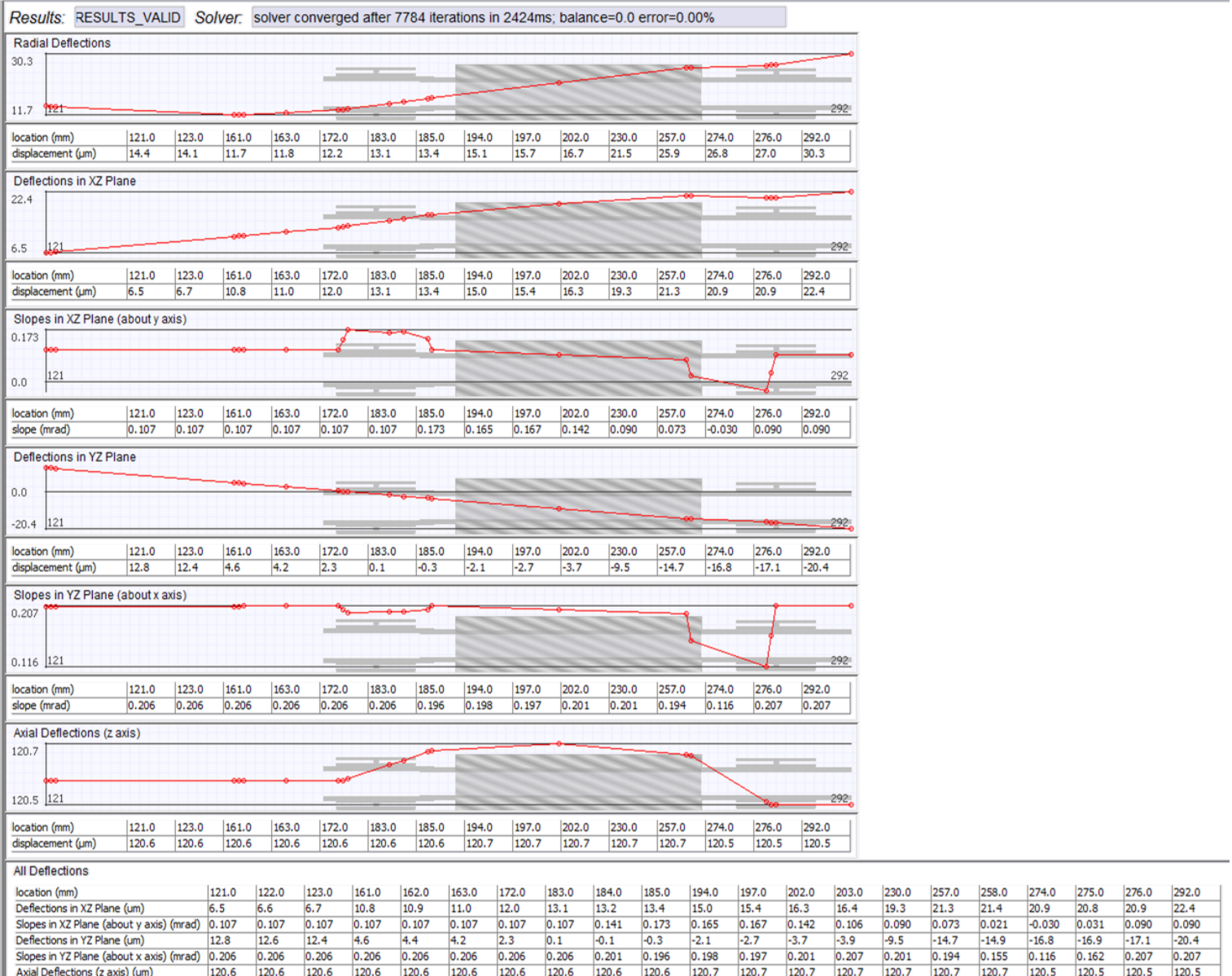


Fig. 62 Slopes and Deflections of the Carrier with Respect to Location

In this case the differential is a very stiff part as well as the carrier shaft, therefore the most deformation is determined by the clearance of the supporting bearings. The combined deformation are still very small, resulting 0.069 mm center distance difference and 0.259 mrad load of action misalignment (LOAMA).



5.4.4. Stresses Applied on Shaft

After the simulation is done ,the results are obtained for the deflection of the Shafts which can be seen in the Table 18.

Tab. 18 The von Misses Stresses Applied on Shafts

Load Case/Shaft	Sun	Differential	Carrier	Planetary Gearset
Nominal Torque	28 MPa	30 MPa	44 MPa	119 MPa
Peak Torque	52 MPa	56 MPa	81 MPa	210 MPa

By this part of the analysis, the areas which may have high stress can be detected. The maximum von Misses stress is acceptable by the Ricardo is 800 MPa that, all of the stress values are within the limits.

After the simulations checked from the software SABR/GEAR, it can be said that the gearbox system is hypothetically ready for production. However, the next iterations would save a lot of weight, cost and reduce the risk of potential failures.

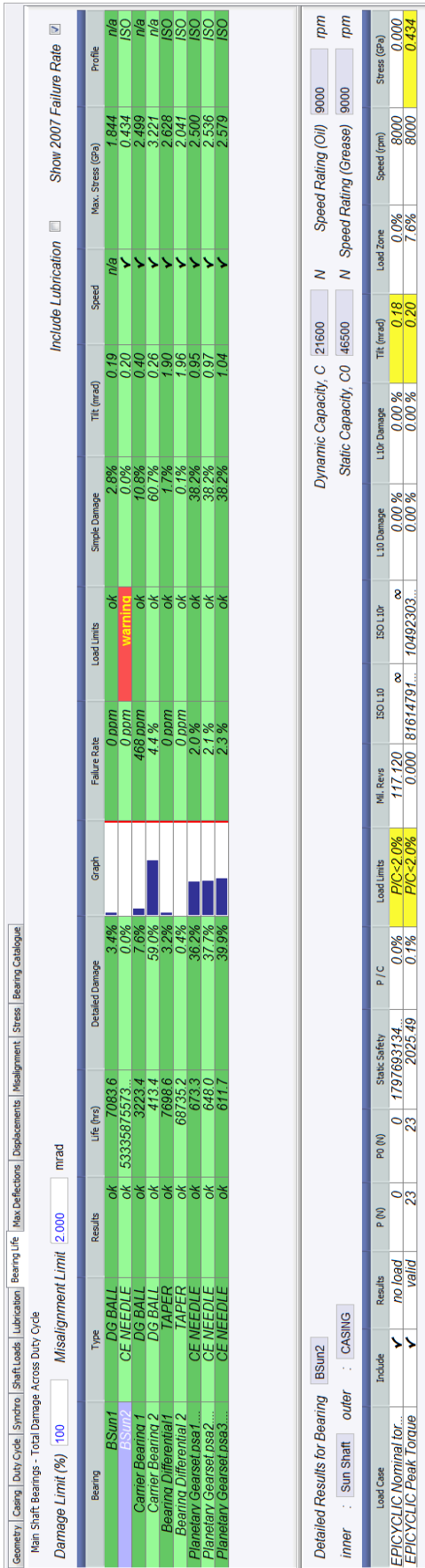


Fig. 64 Life Conditions of Bearings in SABR Software

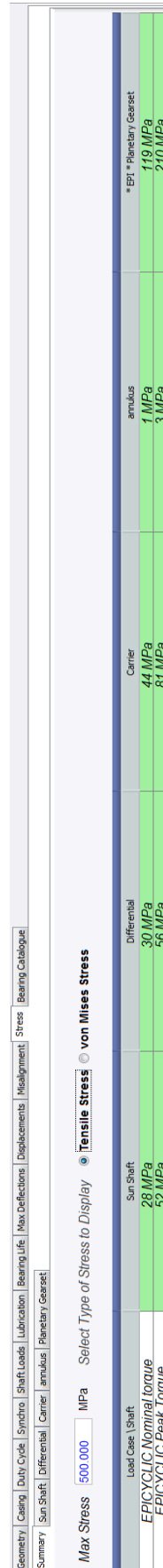


Fig. 63 Results of Stresses Applied on Shafts in SABR Software



6. Conclusion

The task of the thesis was a design a planetary gearbox system for a city car which the range of the electric vehicle is adequate for daily urban activities.

Firstly, the research amongst battery electric vehicles dominating the market was made and their powertrains were analysed to find inspiration and observe the current state of art powertrains. Since the topic of the thesis is designing a planetary gearset for an electric vehicle, the designs with planetary gearsets become the main inspiration for the powertrain which is going to be designed. Also, to be able to observe more complex designs, the patent research was made, from there it was seen that how the planetary reductions are done.

After the battery electric vehicles and the patent research, vehicle parameters are selected, for the city car. For the parameter selection, the closest production vehicle was Chevrolet Bolt EV and the specifications of Chevrolet Bolt EV become the main inspiration vehicle for the design.

To be able to find the total ratio of the powertrain system, longitudinal dynamics calculations were made, the resistance forces have been found. Total gear reduction ratio (i) is calculated in the condition of the maximum speed that, in the vehicle specifications, maximum speed was given approximately 160 km/h, and the total ratio was found as $i=5.6737$.

Before the design process started, it was asked in the thesis to compare several powertrain systems in efficiency, mass and dimension point of view. Two of the designs were planetary gearsets and the third variant was a conventional layshaft transmission. From there the 'Variant 1' is selected as the powertrain to be designed. There are three motivations behind this decision that ; the ground clearance issue, wear of the homokinetic joints and modification of the rotor in the electric motor.

After the variant which is going to be designed is determined, the total ratio is divided between the Planetary Gearset ($i=2.578$) and the Final Drive ($i_{fd}=2.2$). Pitch diameter, number of teeth and dimension calculations are done with the help of mechanical design tables.

The assembly condition of the planetary gearset is checked by the formula and the answer have been found integer, which is a proof of assembly condition was provided.



When the required calculation of the dimensions, the material has been selected for the production. The aimed material for production was the case hardened steel 27MnCr5. The material parameters have been entered to the softwares SABR and GEAR.

Company Ricardo Prague, have recommended a duty cycle for the specific powertrain, which was mentioned under the Chapter 5.3.1, Table 10. The duty cycle have applied in the GEAR Software simulation for determination of Bending and Contact Stress between the meshes, Sun/Planet, Planet/Ring and Pinion/Final Drive.

For the assembly, the bearings are selected on the shaft, which are described under Chapter 5.4.1, Table 15. With the SABR Software, the Bearing Life and Temperatures, Stresses Applied on shafts and Deflections on shafts have been determined in the simulation and the results were obtained.

In conclusion, all of the simultaion results are reasonable and in the limits. Those results shows that the production of the gearset system is possible.



Fig. 65 The Planetary Gearbox For Electric Vehicle in CATIA V5

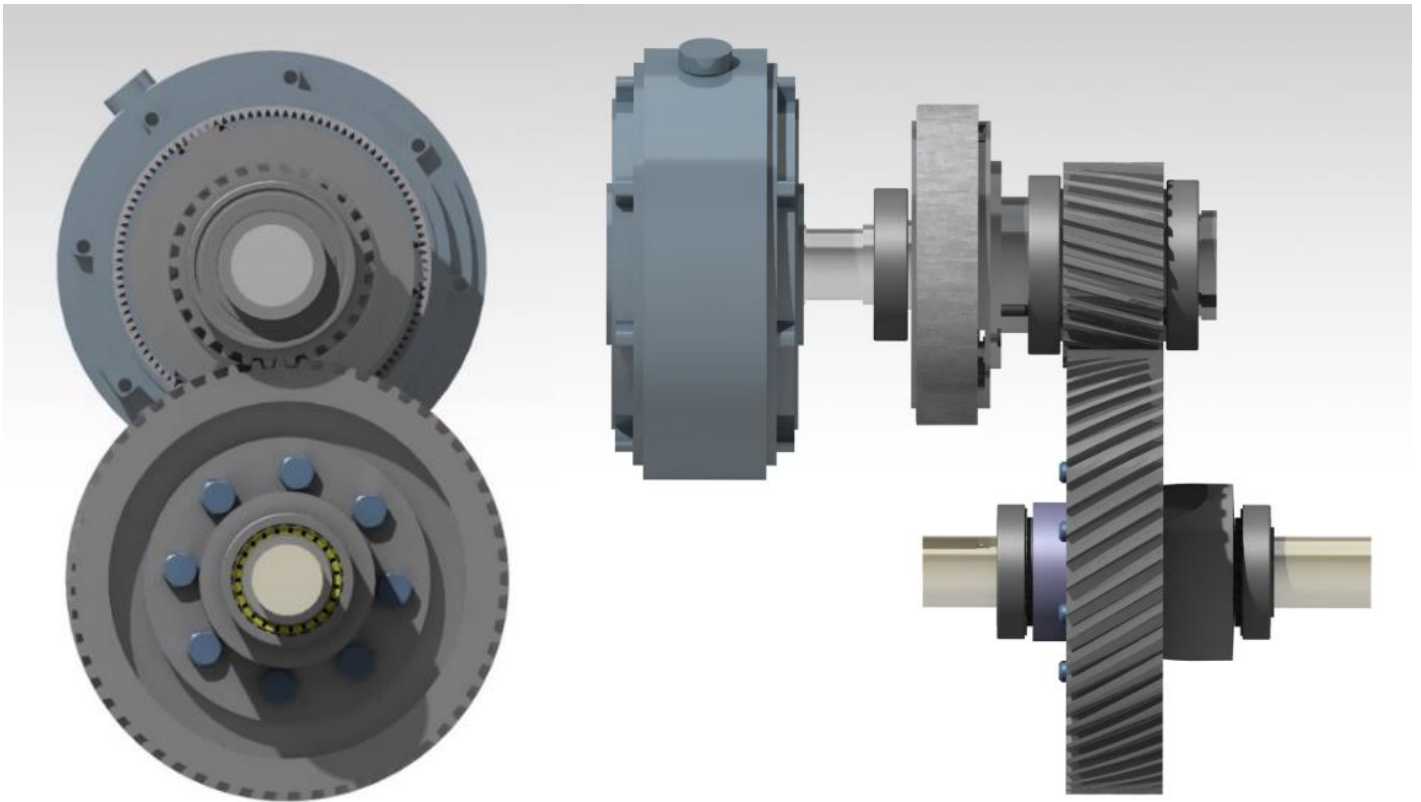


Fig. 66 *Front and Side View Of the Powertrain Design*



7. References

- [1] IEA (2019), "Global EV Outlook 2019", IEA, Paris <https://www.iea.org/reports/global-ev-outlook-2019>*
- [2] E. A. Grunditz, T. Thiringer, "Performance Analysis of Current BEVs Based on a Comprehensive Review of Specifications", IEEE Trans. Transp. Electr., vol. 2, no. 3, pp. 270-289, 2016.
- [3] "Components and Systems for Electric Vehicles (HEVs/EVs)" Hitachi Review 22 November 2018 http://www.hitachi.com/rev/archive/2018/r2018_01/10b02/index.html
- [4] Un-Noor, F.; Padmanaban, S.; Mihet-Popa, L.; Mollah, M.N.; Hossain, E. A Comprehensive Study of Key Electric Vehicle (EV) Components, Technologies, Challenges, Impacts, and Future Direction of Development. Energies 2017.*
- [5] AUDI : Audi e-Tron [online] [cit. 21.03.2020] <https://www.audi.com/en/experience-audi/models-and-technology/production-models/e-tron.html>
- [6] A2mac1.com - Automotive benchmarking [online]. [cit. 2020-03-21]. Available from: www.a2mac1.com
- [7] BMW : BMW i3 [online] [cit. 21.03.2020] <https://www.bmw.com/en/bmw-models/bmw-i3.html>
- [8] Wikipedia : BMW i3 [cit. 21.03.2020] https://en.wikipedia.org/wiki/BMW_i3
- [9] Citroen : Citroen C-Zero
- [10] Chevrolet : Chevrolet Bolt EV [cit. 22.03.2020] <https://www.chevrolet.com/electric/bolt-ev>
- [11] Tesla : Tesla Model 3 [cit. 22.03.2020] <https://www.tesla.com/model3>
- [12] Tesla: Tesla Model S [cit. 22.03.2020] <https://www.tesla.com/models>
- [13] Tesla : Tesla Model X [cit. 22.03.2020] <https://www.tesla.com/models>
- [14] The IPC : https://en.wikipedia.org/wiki/International_Patent_Classification
- [15] The CPC : https://en.wikipedia.org/wiki/Cooperative_Patent_Classification
- [16] Espacenet Patent Research : <https://worldwide.espacenet.com/>
- [17] Patent KR101971189B1, Transmission of Electric Vehicle and the Control Method: <https://worldwide.espacenet.com/patent/search/family/065800652/publication/KR101971189B1?q=KR101971189B1>



- [18] Patent WO2019214995A1, Multi Speed Planetary Transmission for at Least One Electric Machine :
<https://worldwide.espacenet.com/patent/search/family/066625923/publication/WO2019214995A1?q=WO2019214995A1>
- [19] Patent WO2019115204A1, Electric Drive Device for A Motor Vehicle :
<https://worldwide.espacenet.com/patent/search/family/064477153/publication/WO2019115204A1?q=WO2019115204A1>
- [20] Patent WO2019091719A1 , Transmission for an electric vehicle :
<https://worldwide.espacenet.com/patent/search/family/063797379/publication/WO2019091719A1?q=WO2019091719A1%20>
- [21] Patent US20160003351A1, Two-speed transmission for vehicle :
<https://worldwide.espacenet.com/patent/search/family/054866094/publication/US2016003351A1?q=KR20160005209A>
- [22] Chevrolet Bolt Specifications [online] [cit. 15.04.2020]
<https://media.chevrolet.com/media/us/en/chevrolet/vehicles/bolt-ev/2020.tab1.html>
- [23-24] Harald Naunheimer, Bernd Bertsche, Joachim Ryborz, Wolfgang Novak
Automotive Transmissions, Fundamentals, Selection, Design and Application Second Edition
- [25] Harald Naunheimer, Bernd Bertsche, Joachim Ryborz, Wolfgang Novak
Automotive Transmissions, Fundamentals, Selection, Design and Application Second Edition
- [26] Yasa Motors : Yasa P-400 RS Product Sheet [cit. 24.04.2020] https://www.yasa.com/wp-content/uploads/2018/01/YASA_P400_Product_Sheet.pdf
- [27] G. Achtenova, “Planetary Gear Sets in Automotive Transmissions” , ver. 2017 pp.15-18.
- [28] G. Achtenova, “Planetary Gear Sets in Automotive Transmissions” , ver. 2017 pp.16, “sec. 2.5.1 Lubrication Losses”
- [29] G. Achtenova, “Planetary Gear Sets in Automotive Transmissions” , ver. 2017 pp.17, “sec. 2.5.2 Tooth Friction Losses, Table 2”
- [30]] Harald Naunheimer, Bernd Bertsche, Joachim Ryborz, Wolfgang Novak
Automotive Transmissions, Fundamentals, Selection, Design and Application Second Edition, Chapter 4.2.4 Final Ratio
- [31] G. Achtenova, “Planetary Gear Sets in Automotive Transmissions” , ver. 2017 pp.10, ‘definition of negative ratio‘



- [32] Wikipedia :Helix Angle [cit 07.06.2020] https://en.wikipedia.org/wiki/Helix_angle
- [33] Shigley. Shigley's Mechanical Engineering Design. New York: McGraw-Hill, 2011. Chapter 13-10 Parallel Helical Gears*
- [34] Ricardo PLC, SABR/SABR Software [cit. 11.06.2020] <https://ricardo.com/>
- [35] SKF-6209 [cit 08.07.2020] <https://www.skf.com/group/products/rolling-bearings/ball-bearings/deep-groove-ball-bearings/productid-6209>
- [36] SKF-455017 [cit 08.07.2020] <https://www.skf.com/group/products/rolling-bearings/roller-bearings/needle-roller-bearings/needle-roller-and-cage-assemblies/productid-K%2045X50X17>
- [37] SKF-6013Z [cit. 08.07.2020] <https://www.skf.com/group/products/rolling-bearings/ball-bearings/deep-groove-ball-bearings/productid-6013-Z>
- [38] SKF-6012 [cit. 08.07.2020] <https://www.skf.com/group/products/rolling-bearings/ball-bearings/deep-groove-ball-bearings/productid-6012>
- [39] SKF 32009[cit. 08.07.2020] <https://www.skf.com/group/products/rolling-bearings/roller-bearings/tapered-roller-bearings/single-row-tapered-roller-bearings/productid-32009%20>
- [40] SKF-K121812 TN [cit. 08.07.2020] <https://www.skf.com/group/search-results?q=K%2012X18X12%20TN&searcher=all&site=307&language=en>

Attachments

1. CAD Model (2D Autocad, 3D CATIA)
2. Excel Calculations
3. Specifications of Bearings in the Assembly
4. SABR/GEAR Software Solutions
5. Electronic Version of the Thesis